International Journal of Hydrogen Energy 247 (2026) 155851

Contents lists available at ScienceDirect

International Journal of Hydrogen Energy

journal homepage: www.elsevier.com/locate/he

Geospatial and uncertainty-based quantification of Germany's onshore wind-to-hydrogen spatially constrained technical potential

Munzer Osman *, Maria Mercedes Movsessian

School of Business and Economics, RWTH Aachen University, Templergraben 64, Aachen, 52062, Germany

A R T I C L E I N F O

Handling Editor: Dr M Djukic

Keywords:
Wind-to-hydrogen
Levelized cost of hydrogen
Geospatial analysis
Monte Carlo simulation
Germany

A B S T R A C T

This study combines high-resolution geospatial modelling with a 10,000-sample Monte Carlo framework to estimate Germany's wind-to-hydrogen potential and cost distribution. The spatially constrained technical potential centers around 10.8 Mt/year (95% interval: 8.0 - 14.6 Mt/year), representing approximately a 44% reduction compared to deterministic estimates when uncertainty is accounted for. These results reflect an upper-bound spatially constrained technical potential under dedicated onshore wind deployment for electrolysis, excluding system integration and competing electricity demand. Turbine spacing and weather variability are identified as the dominant uncertainty drivers. Low-cost supply is concentrated in northern and coastal regions, with median levelized cost of hydrogen ranging from 7.6 to 18.5 €/kg. Under system-constrained allocation, realizable supply declines substantially; allocating 40% of wind generation to electrolysis yields approximately 4.3 Mt/year, corresponding to only 32 - 46% of projected 2045 demand. These findings indicate that meeting national hydrogen targets will require a diversified renewable supply portfolio.

1. Introduction

Green hydrogen (gH_2) is expected to play a central role in Germany's decarbonization, particularly in industry and system balancing [1]. However, the domestic supply share remains uncertain. The National Hydrogen Strategy [2] projects that 50 to 70% of 2030 demand will be met by imports, with even higher reliance thereafter. Pan-European market modelling [3] indicates that only about 9% of Germany's 2050 demand is supplied domestically. These outlooks underscore the need to quantify realistic domestic gH_2 potential at both national and regional levels. Several studies underscore the value of benchmarking domestic gH_2 potential against imports, particularly under high import-price scenarios. Domestic renewables are not always a cost-saving measure at medium import prices, but they remain a strategic tool for energy security and lower import dependency [4]. This study quantifies Germany's spatially constrained onshore wind-to-hydrogen technical potential at kilometer resolution while propagating geospatial and technical uncertainty.

Germany is Europe's leading wind market, with 66.1 GW onshore installed in 2025 and a target of 115 GW by 2030 [5]. Onshore wind supplied about 25.9% of electricity, and about 15 GW was permitted in 2024 (up 70% year on year) [6]. This policy-driven expansion provides a basis for domestic gH_2 production through direct coupling of new wind capacity with electrolyzers. However, installed capacity alone does not determine hydrogen output. Land-use constraints, regional wind variability, electrolyzer dispatch limits, and EU Renewable Fuels of Non-Biological Origin (RFNBO) rules jointly govern how much certifiable gH_2 can be produced and at what cost. A credible wind-to-hydrogen assessment must quantify regional wind resources together with their spatial links to hydrogen demand hubs and pipeline corridors.

Policy mandates intensify this need. Under the Renewable Energy Directive (RED III), 42% of industrial hydrogen must be RFNBO by 2030, rising to 60% by 2035 [7]. The EU Delegated Act (DA) further enforces additionality and temporal matching so that gH_2 must come from newly added renewable capacity that is demonstrably available when hydrogen is produced [8]. This requires a spatial framework linking resource quality, siting constraints, and certifiable production.

Despite abundant mesoscale wind maps, the translation of kilometer-scale resource data into turbine-scale energy yields and hydrogen output remains insufficiently quantified. Prior German assessments often rely on deterministic setups, sensitivity analyses, or scenario variants, and frequently emphasize hydrogen imports versus domestic economics, supply, or demand outlooks. Where spatial methods are used, they typically prioritize site suitability over uncertainty in energy yields. For

* Corresponding author.
E-mail addresses: munzer.osman@rwth-aachen.de (M. Osman), movsessian@em-dev.rwth-aachen.de (M.M. Movsessian).

https://doi.org/10.1016/j.ijhydene.2026.155851
Received 9 November 2025; Received in revised form 14 May 2026; Accepted 31 May 2026
Available online 4 June 2026

example, H_2PowerD [9] integrates spatial electrolyzer siting with hourly ERA5 and PyPSA but does not provide a national gH_2 potential or a comprehensive spatial uncertainty analysis. Table 1 summarizes relevant studies and highlights how the present work differs in spatial resolution, uncertainty treatment, and reported outputs.

Existing German wind-to-hydrogen assessments primarily rely on deterministic GIS-based potential estimates. These studies provide valuable benchmarks but treat key inputs as fixed or explore limited scenario variants. Specifically, uncertainty in wind variability, land eligibility, turbine parameters, and electrolysis performance is rarely propagated through to national technical potential estimates within a probabilistic framework. To the best of our knowledge, no prior national-scale study for Germany jointly reports probabilistic distributions of both wind-to-hydrogen volumes and levelized cost of hydrogen (LCoH) by combining high-resolution spatial eligibility mapping with Monte Carlo (MC) propagation and dispatch-constrained cost optimization.

This study addresses that gap by combining Multi Criteria Decision Analysis (MCDA) and Geographic Information System (GIS) modeling with a stochastic Monte Carlo (MC) framework to produce probability distributions and confidence intervals for onshore wind-to-hydrogen output, including both production volumes and costs. While previous studies typically focus on either spatial potential mapping or system optimization, this work demonstrates that their integration leads to materially different conclusions regarding the scale, cost, and feasibility of domestic hydrogen production. The contribution lies in the following integrated elements:

- Integrated spatial-probabilistic framework: Kilometer-scale geospatial wind resource assessment is combined with uncertainty propagation and techno-economic optimization. While prior studies (Table 1) typically apply deterministic GIS-based potential mapping or system optimization models independently, this work integrates spatial exclusions, probabilistic resource modelling, electrolyzer sizing optimization, and cost estimation within a consistent framework. This integrated approach indicates that deterministic assessments (e.g., 19.3 Mt/year in this study and 15.9 Mt/year reported by Jung et al. [17]) may overestimate the expected spatially constrained technical potential. When uncertainty in resource and technical parameters is explicitly accounted for, the central estimate (median) decreases to 10.8 Mt/year (95% interval: 8 - 14.6 Mt/year), corresponding to a reduction of about 44%.
- System-level feasibility assessment: Competing electricity demand substantially reduces realizable hydrogen potential below the spatially constrained technical estimates. Scenario-based allocation of onshore wind generation to electrolysis indicates that realizable domestic hydrogen supply declines to approximately 3.2 - 5.4 Mt/year under plausible allocation shares (30 - 50%), compared to a central technical potential of 10.8 Mt/year. For a representative allocation of 40%, supply is about 4.3 Mt/year, corresponding to only 32 - 46% of projected 2045 demand [2]. This structural deficit indicates that domestic production alone is insufficient to meet national hydrogen targets and underscores the need for diversified supply strategies.
- Quantification of uncertainty drivers: Global Sobol sensitivity analysis is applied to identify the relative importance of key parameters including wind variability, turbine spacing, and technical parameters. The findings indicate that turbine spacing and wind variability dominate output uncertainty, while electrolyzer efficiency plays a secondary role.
- Off-grid RFNBO-consistent dispatch and robust spatial cost merit order: Wind and electrolyzer capacities are co-optimized under an off-grid configuration in which electrolyzer dispatch is strictly limited to contemporaneous dedicated wind generation, with no grid exchange. This formulation is consistent with RFNBO principles and yields LCoH estimates representing a conservative, resource-driven upper bound benchmark for hydrogen production costs. Under this configuration, the regional merit order remains stable across all Monte Carlo realizations, with northern and coastal regions consistently occupying the low-cost (7.6 - 9.3 €/kg) segment of the supply curve. This indicates that the cost advantage of northern Germany is primarily driven by underlying resource endowment, and that the supply curve hierarchy is robust under dedicated renewable supply conditions.
- Spatial supply-demand mapping and transport capacity benchmarking: Regional LCoH distributions are aggregated into a national supply curve and benchmarked against hydrogen demand locations and planned transport infrastructure. Static comparison of production volumes with pipeline corridor capacities suggests that transmission infrastructure may constrain the utilization of technically eligible supply in high-production regions. These findings link spatial cost structures to indicative system-level constraints and highlight the importance of infrastructure development for realizing regional production potential.
- LCoH scenario distribution: The LCoH scenario outcomes demonstrate that hydrogen production costs are primarily governed by electrolyzer utilization (full-load hours) rather than unit capital costs. Sensitivity analyses further reveal that financing conditions

Table 1

Key German and EU green-hydrogen studies. Spatial scope, methods, uncertainty handling, and main outputs; differences to this study are highlighted.

Study	Country	Methods	Uncertainty Quantification	Key Outputs
Behrens et al. (H_2PowerD) (2025) [9]	Germany	Spatial clustering, MCDA, PyPSA siting	Deterministic & sensitivities	Optimized electrolyzer sites (no national gH_2 potential, no full spatial uncertainty)
HYPAT/HyPriM [3]	Pan European	Cost-minimizing market model	Deterministic & scenario variants	Least-cost trade flows to meet H_2 demand (country level)
Attiaoui M [10]	Portugal	GIS potential mapping	Deterministic	Wind-to-H_2 atlas (limited uncertainty treatment)
Peterssen F [4]	Germany	Cost-optimized energy system model	Deterministic	Imports vs. domestic expansion potential
Seeger et al. [11]	Germany	Techno-economics & supply chain	Deterministic & scenario variants	H_2Pathway Explorer, LCoH benchmarking
Télessy et al. [12]	Germany	Pipeline integrity/costs	Deterministic & sensitivities	Repurposing gas pipelines for H_2
Wolf et al. [13]	Germany & other regions	Annuity-based LCoH	Stochastic Monte Carlo (MC)	Import vs. domestic cost competitiveness
Alhadhrami et al. [14]	Germany & Saudi Arabia	PLEXOS modeling	Deterministic scenario analysis	H_2 costs from Saudia Arabia to Germany
Eißler [15]	Germany & Australia	Genetic-algorithm PtX planning	Deterministic & scenario variants	H_2 derivatives costs from Australia to Germany
Husarek D [16]	Germany	Multi-modal energy system Linear Programing (LP)	Deterministic & sensitivities	High-resolution German H_2 supply chain
Jung et al. [17]	Germany	Shear wind model, GIS constraints, turbine power curves, electrolysis	Deterministic, uncertainty discussed qualitatively	Technical Wind-to-Hydrogen Potential

(discount rate) exert a more dominant influence on LCoH than moderate variations in electrolyzer CAPEX, identifying financing and regional resource endowment as the principal levers for cost reduction.

These findings extend beyond methodological integration by providing quantitative evidence on the physical, spatial, and economic limits of domestic wind-to-hydrogen systems. While demonstrated for Germany, the framework is transferable to other regions facing comparable resources, land-use, and hydrogen-integration challenges. By generating probabilistic estimates rather than deterministic point values, and releasing all data and code for reproducibility, the analysis enables a more rigorous assessment of uncertainty and system feasibility. The result is a probabilistic, spatially explicit wind-to-hydrogen atlas that contributes to a clearer understanding of the role of domestic production within broader hydrogen supply strategies.

2. Methods

This study aims to comprehensively assess the spatially constrained technical potential for green hydrogen production from onshore wind in Germany. In this study, "technical potential" refers to the maximum hydrogen production achievable under engineering and spatial feasibility constraints, including turbine spacing, land-use exclusions, and environmental restrictions implemented through spatial masks and siting thresholds. These assumptions reflect physical siting feasibility rather than economic or system optimization. The resulting estimates therefore represent a spatially constrained technical potential, positioned between theoretical resource potential and deployable potential that would additionally consider permitting, market conditions, and policy constraints [18]. The technical potential in this study should therefore be interpreted as an upper bound on hydrogen production from spatially eligible onshore wind resources under the stated siting constraints, rather than as a supply projection. Assumptions on electricity allocation to electrolysis and RFNBO compliance are treated as scenario constraints and are not part of the technical potential definition.

In practice, only a fraction of onshore wind generation is likely to be available for electrolysis due to competing electricity demand, system balancing requirements, and the continued operation of the existing wind fleet. In this study, "realizable hydrogen supply" refers to the spatially constrained technical potential that can be achieved under system constraints, including competing electricity demand, as represented through scenario-based allocation assumptions. To address the uncertainty of competing electricity demand, this study employs a scenario-based allocation framework. These scenarios evaluate the varying proportions of onshore wind capacity dedicated to electrolysis versus the general power grid. They quantify how much of the spatially constrained technical potential could be realized under alternative allocation shares. The allocation share is treated as a system constraint informed by literature-based electricity demand projections, rather than a free sensitivity parameter.

The methodology integrates two distinct categories of exclusion criteria: technical constraints and socio-environmental constraints. (*i*) Technical constraints include wind power density (*PD*), elevation, and slope, (*ii*) while socio-environmental constraints include land use and protected areas. The technical wind energy potential is estimated by combining spatial *PD* with wind turbine generator (WTG) characteristics, efficiency, availability, and deployment parameters, including rotor diameter and turbine spacing. Wind energy is then converted to gH_2 using electrolyzer efficiency. In addition to deterministic estimates, a stochastic Monte Carlo (MC) framework captures uncertainty in wind variability, turbine availability, spacing, and electrolyzer performance, yielding probabilistic distributions and confidence intervals of gH_2 output. Beyond volumes, the Levelized Cost of Hydrogen (LCoH) is computed with a Linear Programming (LP) model that co-sizes wind and electrolyzer capacities subject to temporal-matching constraints. The results are further used to construct a gH_2 supply curve, linking production potential to associated production costs. Fig. 1 presents the overall methodological workflow of this study.

The analysis is implemented in Python 3.11 and covers Germany's territory (latitude 47.2° to 55.1° N, longitude 5.9° to 15.0° E), divided into 38 subregions based on Nomenclature of Territorial Units for Statistics (NUTS-2) boundaries. Although results are reported at the NUTS-2 level, the technical potential is derived from spatially explicit geospatial modelling at kilometer resolution. Spatial exclusions, terrain constraints, and wind power density are computed at grid-cell resolution using high-resolution datasets before aggregation to NUTS-2 by area-weighted summation (Table 3). The NUTS-2 framework is used for stochastic parameterization and policy-relevant interpretation, while the underlying resource assessment remains spatially explicit. This approach avoids biases associated with coarse regional averages and preserves realistic land availability estimates, including within-region heterogeneity in exclusions and resource quality.

2.1. Deterministic model

The deterministic model follows established methodologies where output values depend entirely on fixed input parameters [24]. Wind energy potential is first quantified through mean *PD* , which represents the kinetic energy in moving air [25], and is proportional to the cube of wind speed (v). Wind speed variability is modelled using the Weibull distribution, characterized by shape k and scale A, which is widely validated for wind resource studies [26]. Equation (1) gives the Weibull wind speed probability density function. Equation (2) expresses the long-term mean wind power density *PD* in (W/m^2) as a function of the Weibull parameters, air density ρ, and the gamma function Γ.

$$f(v) = (k/A)^* (v/A)^{k-1} {}^* exp^{-(v/A)^k} \tag{1}$$

$$PD(x,y) = 0.5^* \rho^* E[v^3] = 0.5^* \rho^* A^3 \cdot \Gamma(1+3/k) \tag{2}$$

The extractable electrical power density P_e after aerodynamic and system losses considers the theoretical maximum extraction (Betz limit, $\eta_{Betz} = 59.3\%$ [27]) and system conversion losses (η_{sys}).

$$P_e(x,y) = PD(x,y)^* \eta_{Betz}{}^* \eta_{sys} \tag{3}$$

Land-use efficiency, reflecting the land-use utilization factor f_{util} from turbine spacing, is represented by a spacing factor, where the center-to-center spacing φ equals n times rotor diameter D. This yields:

$$f_{util} = \pi(0.5^*D/\varphi)^2 = \pi(2n)^{-2} = 0.785^* n^{-2} \tag{4}$$

The operational power density (P_o) after applying the spacing constraints f_{util} is:

$$P_o(x,y) = P_e(x,y)^* f_{util} \tag{5}$$

The technical mean electrical power density P_t after spatial exclusions incorporates binary masks for land cover, protected areas, elevation limitations, and slope thresholds. This technical wind output is interpreted as mean electrical power density (W/m^2 of useable land) over spatially eligible land:

$$P_t(x,y) = P_o(x,y) \,.\, M_l(x,y) \,.\, M_p(x,y) \,.\, M_e(x,y) \,.\, M_s(x,y) \tag{6}$$

The annual technical wind energy potential $Prod_{total}$ and the technical gH_2 production from wind energy $Prod_{gH2}$ is then defined as:

$$Prod_{total} = \sum_{x,y} P_t(x,y)^* A_{pixel}{}^* h \tag{7}$$

$$Prod_{gH2} = Prod_{total}{}^* \eta_{elec} / 39.39 \tag{8}$$

Where A_{pixel} is the pixel area, h is hours per year, and η_{elec} is the elec-

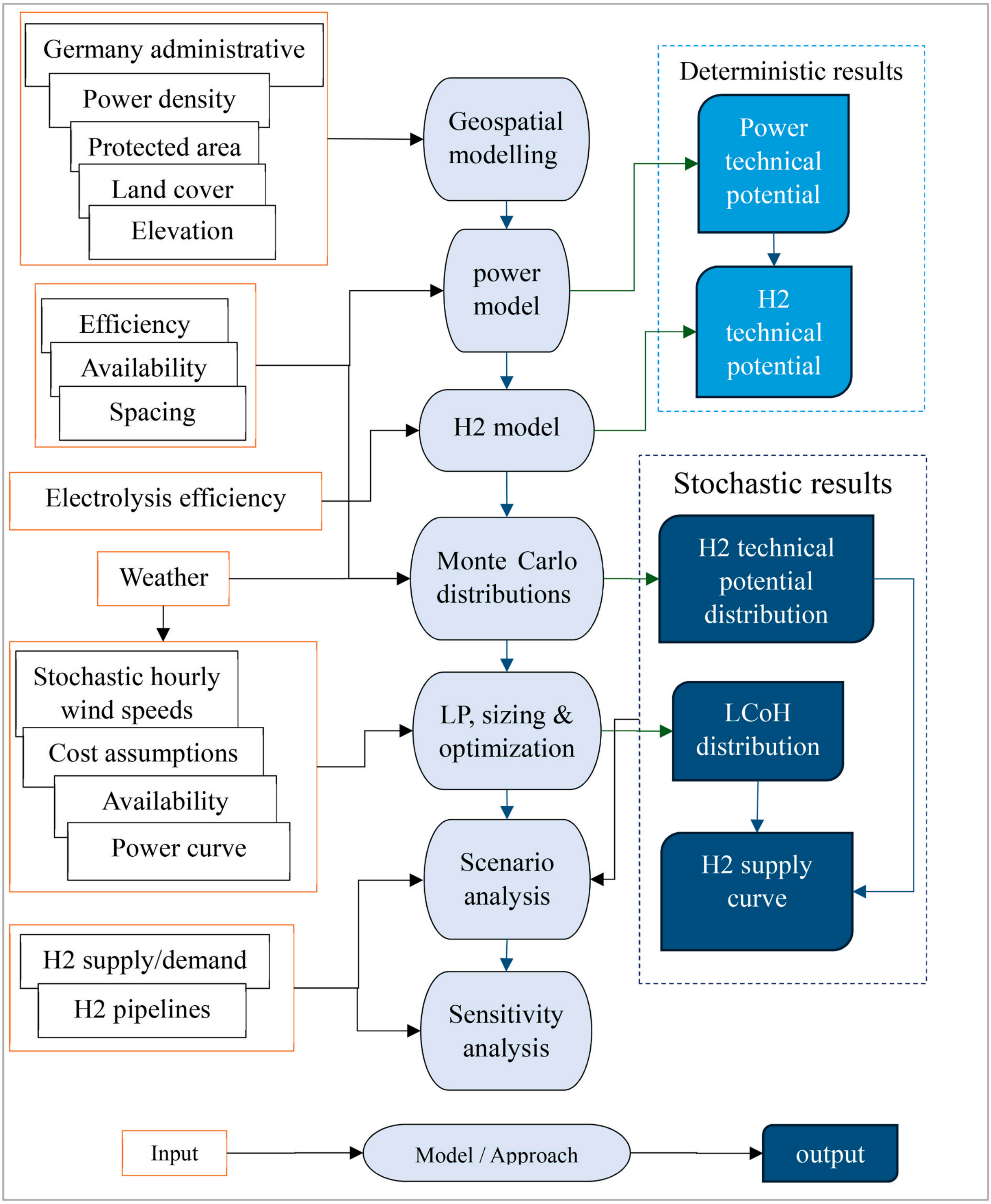

Fig. 1. Methodology workflow of this study, linking geospatial eligibility mapping, deterministic potential estimation, Monte Carlo uncertainty analysis, and Linear Programming-based LCoH and supply-curve construction.

trolyzer efficiency. 39.39 kWh/kg is the higher heating value of hydrogen.

Historical capacity factor estimation: Historical capacity factors are derived from hourly wind-speed time series at NUTS resolution. Wind speeds are mapped to turbine power using a representative Vestas V136-4.0 MW power curve, accounting for cut-in (3 m/s), rated (12 m/s), and cut-out (15 m/s) behavior. For each hour t, the corresponding turbine power $P(t)$ is obtained by interpolating the power curve at the observed wind speed. Annual energy production is then calculated by summing hourly power output over the year, and the capacity factor is computed as,

$$CF_{r,y} = \sum_t P(t)\triangle t \bigg/ P_{rated} T \tag{9}$$

where P_{rated} is the rated turbine capacity (4 MW) and T is the total number of hours in the year. Regional capacity factors are averaged across years to obtain long-run regional CF estimates. These regional

Table 2
Stochastic model parameter distributions, settings, and effective ranges used in the nested Monte Carlo-QMC simulation framework.

Parameter	Distribution	Parameters	Range	Description
Power density scale perturbation	Truncated Normal	Regional variation	0.3 - 1.7	Multiplicative perturbation of Gamma scale parameter for wind power density
Wind power density	Gamma	Regional shape & scale	>0	Region-specific wind resource distribution
Turbine efficiency	Beta (scaled)	a = 8, b = 8, loc = 0.32, scale = 0.10	0.32 - 0.42	Conversion efficiency from wind power density to electrical output
Availability factor	Beta (scaled)	a = 2, b = 5, loc = 0.92, scale = 0.07	0.92 - 0.98	Operational availability of wind turbines
Turbine spacing	Triangular	min = 5D, mode = 7D, max = 10D	5 -10 rotor diameters	Turbine spacing determining installable capacity density
Electrolyzer efficiency	Truncated Normal	μ = 0.70, σ = 0.03	0.65 - 0.85	Electrical-to-hydrogen conversion efficiency
Random seed	-	-	42	Random seed fixed at 42

Table 3
Spatial input datasets used for wind energy technical potential assessment, including source, resolution, and temporal coverage.

Dataset	Source	Resolution	Temporal Coverage	Variable
Wind Power Density	Global Wind Atlas (GWA) [19]	250 m	2008 - 2017	Power density at 100 m (W/m^2)
Land Cover	ArcGIS-Esri/Microsoft Annual Land Cover [20]	10 m	Annual	10-class land cover
Protected Areas	WDPA 2025 [21]	Vector polygons	1819 - present	Conservation zones
Digital Elevation	EuroDEM 2023 [22]	60 m	2023	Elevation (m), ±8 - 10 m vertical accuracy
Slope	Derived from EuroDEM	60 m	-	Slope (degrees)
Wind Speed (historical)	ERA5 reanalysis [23]	~250 m	1979 - 2025	Hourly wind speed at 100 m

values are subsequently aggregated to derive a national long-run capacity factor (26.7%) used for benchmarking and to express the deterministic PD-based mean power in equivalent nameplate GW for comparison with policy capacity targets.

This workflow directly links spatially explicit wind resource availability to hydrogen production estimates, enabling consistent assessment of wind-to-hydrogen pathways.

2.2. Stochastic model

To account for inherent uncertainties in wind-to-hydrogen systems, the stochastic framework models variability across five dimensions: weather variability, turbine efficiency, turbine availability, land-use intensity (spacing), and electrolyzer performance.

i. *Weather variability:* Wind *PD* variability is modelled using a gamma distribution fitted to historical *PD* data (2014 - 2024) at the NUTS-2 level, consistent with established practices in the literature. The gamma distribution is widely used for modelling non-negative, right-skewed energy-related variables and provides a flexible representation of wind resource variability across spatial scales [28]. Interannual variability is incorporated by perturbing the scale parameter (θ) of the fitted distribution. Perturbing θ rather than α ensures that variability primarily affects the mean resource level while preserving the distributional shape, consistent with observed interannual wind

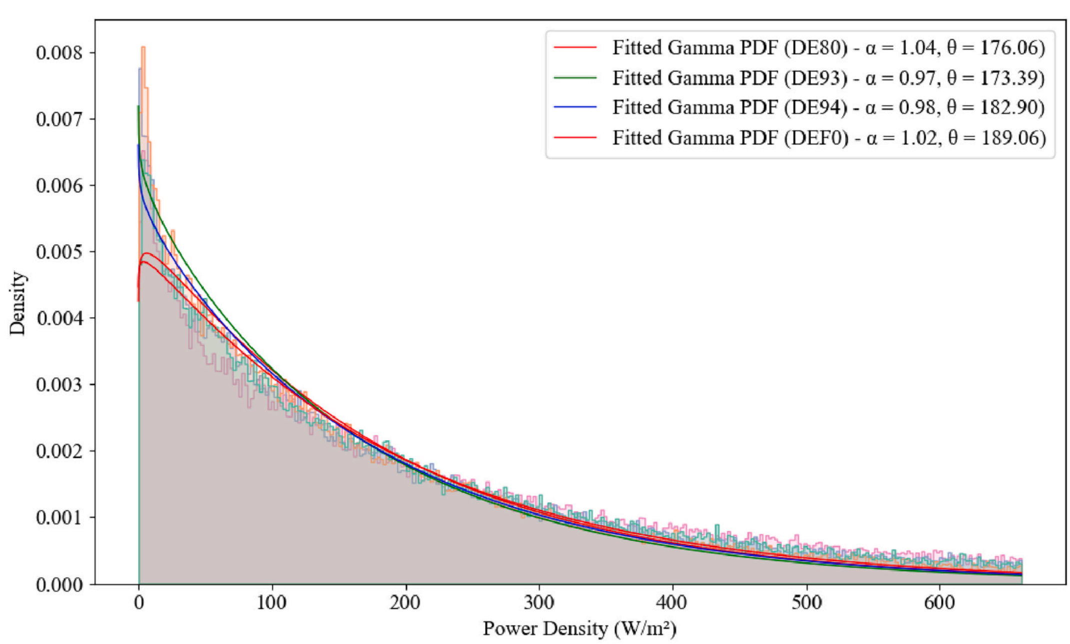

Fig. 2. Gamma distribution fits to historical wind power density (PD) (2014 - 2024) for four NUTS-2 regions. Scale perturbation via QMC sampling is used to generate plausible PD ensembles.

variability patterns. The perturbed scale parameter ($\theta_{pert,i}$) is defined as:

$$\theta_{pert,i} = mean(\theta_i) \cdot \epsilon_i \tag{10}$$

$$\epsilon_i = 1 \pm (\sigma_\theta / mean(\theta_i)), \epsilon_i \sim \mathscr{N}(1, (\sigma_\theta / mean(\theta_i))) \tag{11}$$

where ϵ_i represents a multiplicative perturbation factor sampled from a normal distribution $\mathscr{N}$ centered at 1 with standard deviation $(\sigma_\theta / mean(\theta_i))$ calibrated to the historical dispersions. This formulation ensures that sampled scenarios remain physically consistent and bounded within empirically observed variability ranges. Fig. 2 illustrates gamma fits for four exemplary NUTS-2 regions.

Quasi-Monte Carlo (QMC) Sobol sequences [29] are then used to efficiently sample the perturbed distributions. Uniform samples u_i are transformed via the inverse cumulative distribution function of the gamma distribution:

$$\widehat{X}_i = F_\Gamma^{-1}(u_i\ ;\ \alpha, \theta_{pert,i}) \tag{12}$$

Where u_i is a random sample, and F_Γ^{-1} is the quantile function of the gamma distribution. This process is repeated for n samples.

This approach enables low-discrepancy sampling while preserving the statistical properties of the fitted distributions. The resulting ensemble captures spatially resolved, physically consistent, and statistically grounded representations of wind resource uncertainty.

ii. *WTG efficiency (power coefficient):* The WTG energy output is fundamentally constrained by physics. According to Betz's law, the maximum theoretical efficiency of WTG (i.e., the power coefficient) is limited to 16/27, or approximately 59.3% of the kinetic energy in the wind [27]. Under optimal conditions, efficiency values of 0.397 and 0.425 are found in the literature [30] [31]. Depending on WTG design, aerodynamic characteristics, and environmental and technical conditions, the power coefficients can range between 0.30 and 0.45. To account for this technical variability, this study models WTG efficiency using a beta distribution spanning from 0.32 to 0.42, with most values clustering between 0.38 and 0.40.
iii. *WTG availability:* Improvements in monitoring and maintenance practices have contributed to consistently high availability rates for onshore wind farms. For instance, Landini [32] stated an average technical availability ranging between 96% and 98%, excluding grid-related downtime. Similarly, Sunder and Kesavan [33] considered additional failure and repair rates, reporting WTG availability between 94.45% and 99%. To account for broader uncertainty factors in real-world conditions, such as variability in maintenance quality, environmental factors, aging, and unforeseen mechanical failures, this study models availability between 92% and 98% via a beta distribution.
iv. *Area utilization & WTG spacing:* Uncertainty in WTG spacing affects land-use efficiency and energy potential; tight spacing increases wake losses, while wide spacing lowers density and raises land demand. To balance land use and energy efficiency, wind farms typically space WTGs 3 - 5 rotor diameters spanwise and 5 - 9 diameters streamwise, depending on terrain and wind conditions [34]. Other studies suggest increasing streamwise spacing to 10 - 15 diameters to reduce wake losses [35]. This study models uncertainty in rotor spacing using a triangular distribution with a minimum of 5D, a maximum of 10D, and a mode of 7D, reflecting typical industry practices.
v. *Electrolysis efficiency*: Electrolyzer performance significantly influences hydrogen output and varies by technology. IRENA [36] reported electrolyzer system efficiencies of 67% for Proton Exchange Membrane (PEM) and 76% for Alkaline (ALK) technologies in 2017, projecting improvements to approximately 75% and 80%, respectively, by 2025. The DOE [37] reported current efficiency ranges of 72% for low-temperature and 83% for high-temperature electrolysis systems, with targets of 85% and 93% over the long run. In this study, electrolyzer efficiency is sampled from a truncated normal distribution with a mean of 70%, standard deviation of 3%, and bounds of 65% to 85%. Electrolysis is represented as an aggregated conversion process to focus the analysis on spatial wind resource variability and land-constrained while maintaining computational tractability at national scale. Technology-specific operational characteristics, including start-up dynamics, degradation rates, replacement cycles, and differentiated capital costs, are not explicitly modelled; instead, their effects are implicitly captured through the stochastic efficiency distribution. Consequently, the resulting hydrogen production and LCoH estimates reflect a simplified representation of electrolysis performance rather than technology-resolved system behavior. The electrolyzer efficiency was defined at the system level, including balance-of-plant consumption. A baseline efficiency of 70% (HHV) was adopted, representing a conservative yet realistic estimate within literature-reported values [38], [39]. This value was applied consistently across deterministic, stochastic, and demand-scenario analyses to ensure methodological coherence. In the Monte Carlo framework, efficiency was sampled over a bounded range (65 - 85%) to reflect operational variability and potential technological improvements, while maintaining a central tendency aligned with the baseline assumption.

Table 2 summarizes the main MC parameters, distributions, and settings used in the nested MC-QMC simulation framework.

2.2.1. *Sobol sensitivity analysis*

To assess the influence of input variables on gH_2 production, Sobol's global sensitivity analysis is applied. This variance-based method quantifies the contribution of each input, both individually (first-order effects S_1) and in combination with others (total-order effects S_t), to the overall output variance [40]. This offers a rigorous framework for evaluating parameter importance across the full input space. For Sobol sensitivity analysis, a uniform distribution across plausible parameter ranges is adopted, as required by the Saltelli [41] sampling method. While the MC model uses more realistic distributions (e.g., beta, normal, triangular), the uniform assumption enables global sensitivity estimation consistent with the variance-based decomposition framework.

2.2.2. *Optimal sizing, stochastic LCoH calculation & sensitivities*

To capture uncertainty in renewable availability, stochastic hourly wind power profiles are generated for each NUTS-2 region by combining perturbed Weibull distributions, stochastic power curves, and availability (Table 2). To ensure methodological consistency, both the PD-based Monte Carlo potential analysis and the stochastic hourly generation model rely on the same regional wind statistics derived from the historical wind-speed dataset. The potential assessment uses Monte Carlo samples of wind power density, while the operational model uses synthetic hourly wind-speed series parameterized with the same regional Weibull parameters.

Power-curve uncertainty (Fig. 3) is represented by perturbing the partial-load region (3 - 12 m/s) while maintaining the rated power limit (4 MW for V136-4). For each replicate, a 20-year hourly sequence is simulated to reflect inter-annual climate variability, turbine performance, and downtime.

To approximate RFNBO-style temporal matching while maintaining computational tractability across regions and MC realizations, each synthetic hourly wind-availability series is compressed into a binned duration curve for each year (60 bins per year). For year t, each bin b represents an availability level $\bar{a}$ and a duration $h_{t,b}$ (hours), obtained from sorted hourly availability values such that $\sum_b h_b$ and the annual

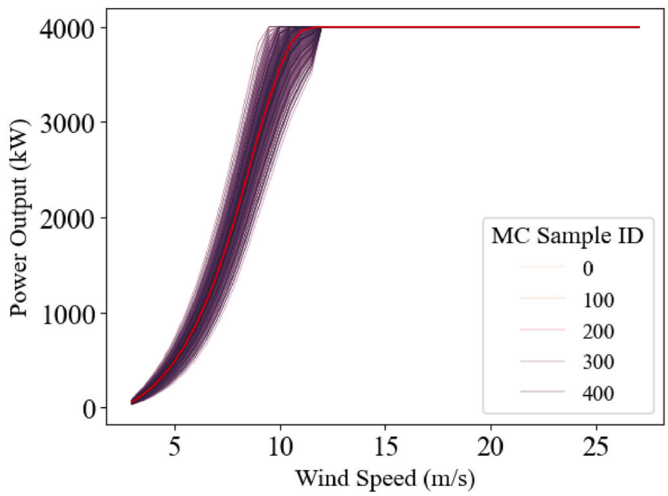

Fig. 3. Monte Carlo perturbation of the wind turbine power curve (n = 500). Grey lines represent perturbed realizations in the partial-load region (3 to 12 m/s); red line denotes the baseline power curve. Rated power is preserved across all samples (scale = 0.2, a = 0.50, seed = 42). (For interpretation of the references to colour in this figure legend, the reader is referred to the Web version of this article.)

energy distribution of wind availability is preserved. The LP then enforces $p_{t,b} \leq \bar{a}w$ and $p_{t,b} \leq E$, where $p_{t,b}$ is electrolyzer dispatch in bin b and year t, w is wind capacity, and E is electrolyzer nameplate capacity. The hydrogen production in year t accumulates over bins as $\sum_b p_{t,b} h_{t,b} \eta_{el}$.

Multiple RFNBO-compliant system configurations exist [8]: Off-grid configuration, where the installation producing electricity is not connected to the grid. Grid-connected systems, where electrolyzers may access electricity from the grid under defined regulatory conditions, including additionality, temporal correlation requirements, and, in some cases, exemptions linked to high renewable penetration in the electricity system. The study adopts an off-grid configuration in which electrolyzer operation is fully constrained by dedicated wind generation. This formulation provides a transparent and physically consistent representation of renewable-constrained hydrogen production, without reliance on grid interactions or market-based dispatch. This configuration is RFNBO-consistent.

Casas Ferrús et al. [42] showed that strict temporal matching without grid interaction, effectively equivalent to an off-grid RFNBO configuration, is associated with higher LCoH due to limited operational flexibility. Introducing grid connection, even in the form of constrained low-price electricity imports, can increase flexibility, reduce overbuild and storage requirements, and thereby lower LCoH. Accordingly, the off-grid formulation adopted in this study represents a conservative benchmark in which hydrogen production is strictly limited by local renewable availability. The resulting LCoH can therefore be interpreted as a resource-driven upper bound under dedicated renewable supply, independent of grid dynamics or market-based dispatch. This approach is consistent with the objective of the study, which focuses on spatially constrained resource assessment rather than full system-dispatch modelling.

Because the model contains no inter-temporal constraints (i.e., no storage state variables, ramping limits, minimum-load constraints, grid exchange, or price-driven dispatch), electrolyzer operation is determined solely by instantaneous wind availability and installed capacity. Under these assumptions, the optimal system sizing depends on the distribution of availability levels rather than their chronological sequence. Sorting hourly availability into duration curves therefore preserves the feasible production set and yields the same optimal capacities and LCoH as the explicit hourly formulation up to numerical tolerance. The duration-curve formulation substantially reduces computational burden. The explicit LP hourly formulation is computationally intensive when combined with 20-year synthetic profiles and 500 Monte Carlo realizations across 38 NUTS-2 regions. While feasible, it substantially limits the breadth of uncertainty sampling. The duration-curve formulation reduces dimensionality without altering the feasible production set under the model assumptions, enabling more extensive uncertainty propagation and sensitivity analysis within the same computational budget. A sensitivity check was performed by comparing the duration-curve LP with the explicit-hourly LP formulation for representative NUTS-2 regions and weather realizations. Across tested NUTS-2 regions and weather realizations, differences in optimal w/E, and LCoH remain below 1%.

The techno-economic LP co-optimizes wind capacity (w) and electrolyzer capacity (E) over a 20-year horizon with decision variables of w, E, and the electrolyzer dispatch per bin per year is $p_{t,b}$. The dispatch is limited by available wind power $\bar{a}$ and by electrolyzer capacity E and consistent with RFNBO-style. A wind-to-electrolyzer build ratio cap $k = 6$ is applied. Annual hydrogen delivery must meet a specified demand D_t each year. The objective function is to minimize the present value of total system costs:

$$min_{E,w,p}\ C_E E + C_w w + \psi C_E E.DF_{10} + \sum_{t=1}^{20} (O_E E + O_w w)(1+g)^{t-1} / (1+r)^t \tag{13}$$

Subject to

$$\begin{aligned} p_{t,b} &\leq E, \forall t, b \\ p_{t,b} &\leq w\,\bar{a}, b \forall t, b \\ w &\leq kE \\ \eta_{el} \sum_b h_{t,b} p_{t,b} &\geq D_t \end{aligned} \tag{14}$$

where C_E, C_w are the specific capital costs (CAPEX), ψ the electrolyzer mid-life replacement fraction, O_E, O_w are annual operating costs (OPEX), r is the discount rate, g is the OPEX escalation rate, DF_{10} the discount factor in year 10, and η_{el} is the efficiency.

This study assumes a base-case CAPEX of 2500 €/kW and wind turbine CAPEX of 1300 €/kW. Annual OPEX is set at 3% of CAPEX, with an escalation rate of 1.5% per year to account for inflationary pressures over the project lifetime. A mid-life stack replacement is assumed at year 10. The base-case discount rate is 6%, consistent with empirical estimates of renewable energy project financing costs in Europe [43].

Furthermore, to assess the sensitivity of LCoH to financing and capital cost uncertainty, 7 CAPEX levels and 5 discount rates are examined, yielding 35 parameter combinations applied over four representative NUTS-2 regions. Reported PEM CAPEX has historically ranged from about 2000 to 5000 USD/kW for small-scale systems, with projections suggesting substantial reductions for large-scale plants [44]. However, potential cost decline depends on system structure. Approximately 15 - 20% of CAPEX is attributable to stack components, which offer meaningful innovation-driven reduction potential, while 25 - 30% corresponds to balance-of-plant equipment with more limited cost flexibility. A significant share (>50%) reflects engineering, procurement, and construction, which remain elevated due to first-of-a-kind project risks and limited standardization [45]. Given these structural constraints and uncertainty in long-term projections, this study adopts a conservative CAPEX range of 2000 to 2750 €/kW in increments of 125 €/kW for sensitivity analysis, representing the lower end of current reported costs while allowing for moderate learning effects. The discount rate range spans typical public financing conditions (2 to 4%) to private or risk-adjusted capital costs (6, 8, and 10%), consistent with hydrogen project financing assumptions in the European context.

By integrating stochastic wind generation, duration-curve compression, and multi-year cost optimization, the framework captures interannual variability while remaining computationally tractable. Results were evaluated across 500 regional scenarios, yielding both average and distributional estimates of LCoH rather than a single deterministic value.

The LP is implemented in Pyomo and solved using Gurobi (version 12.0.3). The LP model is solved using the barrier method. Key solver parameters are set as follows: Method = 1 (barrier), Presolve = 2, Crossover = 0, Feasibility Tolerance = $1e^{-6}$, and Optimality Tolerance = $1e^{-6}$.

2.2.3. Scenario analysis

Targeted scenarios are constructed by selecting subsets of samples on key drivers highlighted by the sensitivity analysis. Two examples are a high-efficiency technology subset, where turbine efficiency, electrolyzer efficiency, and availability exceed their 75th percentiles, and a wide-WTG-spacing subset, where spacing exceeds its 75th percentile. These subsets illustrate how technology and layout choices shift gH_2 outcomes while staying within the stochastic envelope.

2.2.4. Benchmarking pipeline capacity and regional adequacy

The infrastructure representation is intentionally simplified, as large-scale hydrogen supply, demand, and transport networks are not yet fully realized. Instead, indicative supply–demand distributions and projected pipeline developments are used to identify plausible spatial trends and potential transport requirements. Comparing the nominal spatially constrained technical potential (regionally) with indicative transport capacities provides a first-order assessment of potential corridor bottlenecks. This approach therefore represents a high-level evaluation of foreseeable transport adequacy relative to potential hydrogen production. The results should be interpreted as indicative capacity benchmarking under steady-state conditions rather than as a detailed assessment of operational feasibility (i.e., network flow optimization, storage buffering, linepack, or competition with imports are not modelled in this study).

The locations of hydrogen supply and demand are derived from the European Clean Hydrogen Alliance Germany subset [46], and the German Hydrogen Core Network application (BNetzA) [47]. Assets are classified as electrolyzer injection points, import or terminal entries, industrial offtakers, and storage sites. Those values are used without conversion when capacities are given directly in mass units. If only the nameplate electrolyzer capacity is provided and no annual production is stated, the nameplate value is treated as an injection limit, and full-load hours are not inferred. Duplicates are removed by matching project names, coordinates, and operators. Each asset is mapped to its state (Bundesland) by spatial join, and project values are aggregated to state-level injection and offtake totals to obtain supply and demand balances.

Existing and planned pipeline links are digitized as connections between these state nodes. For each link, published hydrogen transport capacity is recorded in kilotons per day; if a source reports energy units, capacities are converted using 39.39 kWh per kg. Links without published capacities are flagged as unknown in the base case. A sensitivity case also applies a placeholder capacity of 120 MWh/day for such links (converted on the same basis). Interregional flows are then benchmarked against the stochastic technical supply with a static adequacy check: state-level surpluses are routed to deficit states along available links subject to corridor limits, and any unserved surplus or unmet offtake is marked as a potential bottleneck together with the constraining link and the affected states.

This simplified infrastructure representation is intended to provide a screening-level assessment of spatial supply, demand mismatches at the national scale. The objective is not to simulate detailed network operation or optimize flows, but to identify structural imbalances between resource availability and demand.

2.3. Data collection

This subsection summarizes the datasets, spatial resolutions, reference periods, and pre-processing steps used in the analysis.

2.3.1. Geospatial

The technical hydrogen potential assessment uses openly available geospatial datasets aggregated to NUTS-2 regions (Eurostat, 2024) [48]. The study area covers approximately 357,600 km^2. Land cover (ArcGIS-Esri, 10 m) [20], protected areas (WDPA-2025) [21], and terrain data (EuroDEM 2023) [22] define exclusion zones and suitability masks. Thresholds include >1 km urban buffers, slope >6°, and elevation >1200 m. These thresholds are more conservative than typical values reported in the literature [49]. These spatial filters ensure realistic wind turbine siting. Table 3 summarizes the geospatial data used in this study.

Similarly, Table 4 summarizes the land cover classes, assigned suitability weights, and inclusion criteria applied in the spatial exclusion analysis.

2.3.2. Wind resource

Wind resource data are obtained from the Global Wind Atlas [19] (ERA5-based, downscaled to 250 m) and complemented with hourly ERA5 reanalysis [23] (1979 - 2025) at 100 m height to capture inter-annual variability. Wind power density *PD* (W/m^2) is calculated assuming an air density of 1.225 kg/m^3 and aggregated to the NUTS-2 level. Fig. 4 shows that the coefficient of variation (CV) of long-term PD ranges from 10 to 16%. Coastal regions (e.g., DEF0, DE60, DE80) show high mean PD and low variability, whereas inland regions (e.g., DE13, DE21, DE27) show greater variability. This variability metric informs the stochastic parameterization.

Overall, this methodological framework links high-resolution geospatial data with stochastic modelling to quantify uncertainty in wind-to-hydrogen conversion. It moves beyond deterministic estimates and provides a more robust assessment of Germany's technical gH_2 potential. The results support planning of renewable expansion, infrastructure, and hydrogen integration strategies.

Data and code, including scripts for geospatial preprocessing, Monte Carlo sampling, and the LP model, are available in a Git repository together with environment files, random seeds, and data sources. Version information for Python and key libraries is provided in the

Table 4
Land cover classification, suitability weights, and inclusion criteria applied in the spatial exclusion analysis.

Layer	Criterion	Threshold/Rule	Outcome
Land cover - Water	Excluded	Weight = 0	Removed
Land cover -Trees/ Forest	Excluded	Weight = 0	Removed
Land cover - Urban/Built	Excluded	Weight = 0	Removed
Land cover - Snow/ Ice	Excluded	Weight = 0	Removed
Land cover - Cloud-covered	Excluded	Weight = 0	Removed
Land cover - Crops	Partial inclusion	Top 20% by suitability	Weight = 0.2
Land cover - Flooded Vegetation	Partial inclusion	Top 30% by suitability	Weight = 0.3
Land cover - Bare Ground	Fully included	Weight = 1	Retained
Land cover - Rangeland/ Scrub	Fully included	Weight = 1	Retained
Urban setback buffer	1 km uniform buffer	National (proxy for local rules)	Excluded within 1 km
Protected areas (WDPA)	Full exclusion	All categories	63% of Germany excluded
Elevation	Upper threshold	>1200 m excluded	High-altitude areas removed
Slope	Upper threshold	>6° excluded	Conservative (literature: up to 9°)

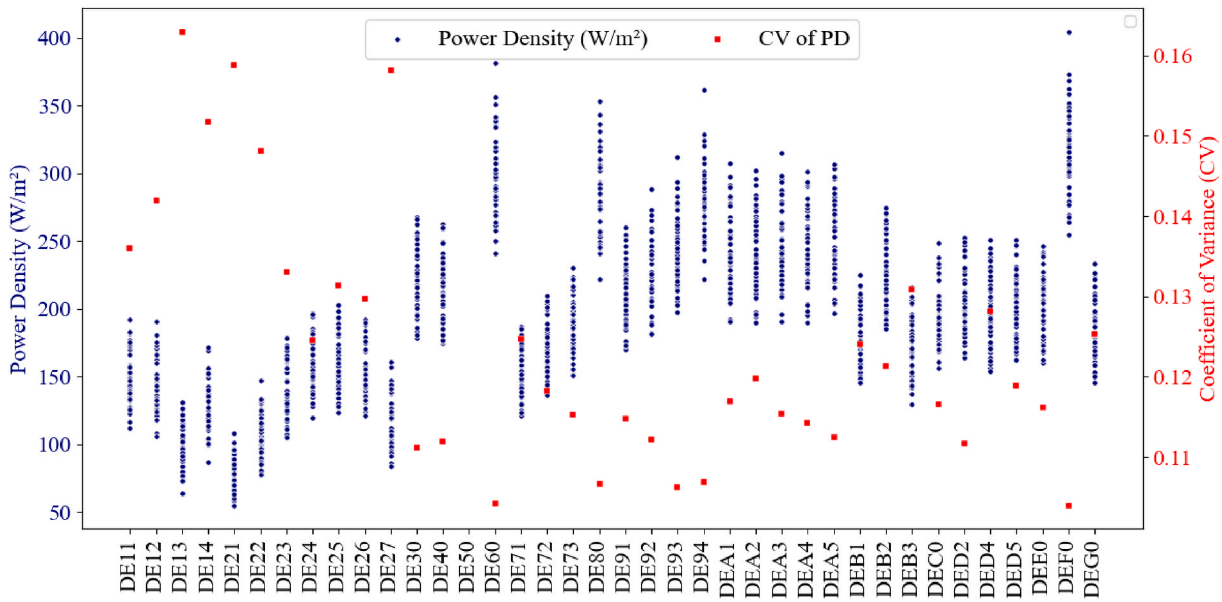

Fig. 4. Annual mean wind power density (*PD*) and coefficient of variance (CV) quantifying interannual variability across Germany's NUTS-2 regions (2014 - 2024).

repository.

3. Results

This section first presents deterministic estimates of Germany's onshore wind energy and gH_2 production, based on fixed technical parameters. These baseline results are complemented by stochastic Monte Carlo (MC) simulations that introduce parameter variability and quantify uncertainty through probabilistic distributions. Resource quality is then translated into levelized costs and a national supply curve. Finally, spatial supply is benchmarked against indicative demand and transport capacity.

3.1. Deterministic model results

Using fixed parameters (WTG efficiency 40%, availability 85%, rotor diameter 150 m, and spacing 800 m or 5.3D), Germany's theoretical onshore wind potential based on power density is about 9719 TWh/year (Fig. 5a). This corresponds to an average output of about 1.11 TW and approximately 4.2 TW of nameplate capacity at a 26.7% capacity factor (1979 - 2024). Applying land-use constraints reduces potential to about 2059 TWh/year (Fig. 5b), a 79% decline. This highlights the importance of spatial constraints and regulatory conditions in shaping estimates of resource potential.

Reductions are heterogeneous across regions (Fig. 6). Southern regions such as Bavaria (e.g., Niederbayern 97.4%, Oberpfalz 96.6%,

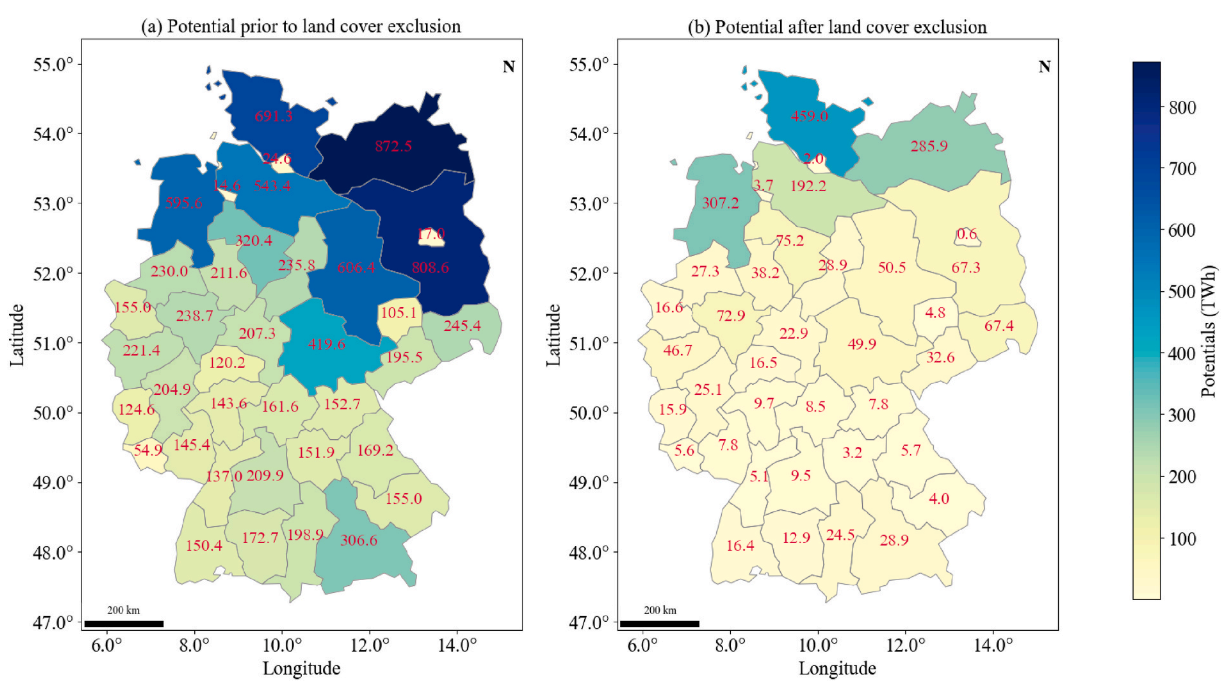

Fig. 5. Theoretical and land-use-constrained onshore wind potential. (a) National theoretical potential derived from power density before exclusions. (b) Potential after applying land-cover constraints. Values are annual TWh; inputs use the fixed technical parameter set described in the text.

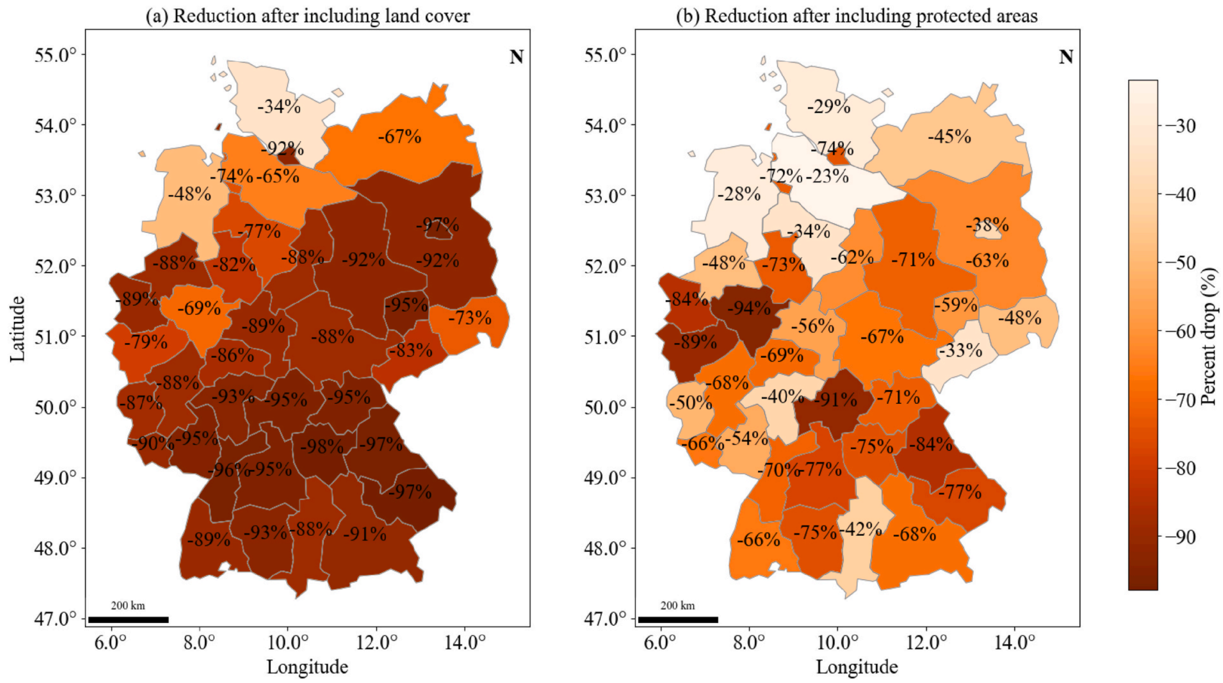

Fig. 6. Regional reduction in technical wind potential due to exclusions. (a) Percentage reduction after land-use constraints. (b) Additional percentage reduction after protected-area constraints. National decline relative to land-use only is 44%; values are shown at NUTS-2.

Mittelfranken 97.9%) and Baden-Württemberg (Karlsruhe 96.3%, Stuttgart 95.5%), experience the largest losses (>95%), driven by dense settlement, forests, and existing designations. Central and eastern areas such as Berlin (96.6%) and Leipzig (95.4%) show similar reductions. In contrast, northern regions retain more potential (e.g., Schleswig-Holstein 33.6%, Weser-Ems 48.4%), reflecting greater land availability and favorable siting. Adding protected areas further lowers the national spatially constrained technical potential to 1149 TWh/year (a 44% decrease relative to land-use-only), with the strongest additional impacts in the south and west (e.g., Unterfranken, Niederbayern, Oberpfalz; Arnsberg, Köln, Düsseldorf). Northern regions show comparatively smaller incremental losses (e.g., Schleswig-Holstein 29.1%, Weser-Ems 28.3%, Lüneburg 23.4%), while parts of the east (Mecklenburg-Vorpommern 45.3%, Brandenburg 62.9%) are moderately affected by Bird Directive sites. Incorporating terrain slope greater than 6° yields a further reduction to about 1086 TWh/year (−5.4%). Sensitivity to the slope threshold is notable. A 4° limit reduces potential by 8.5%. Effects are small in northern plains but larger in the complex terrain of southern and central Germany.

Assuming 70% electrolyzer efficiency, the national spatially

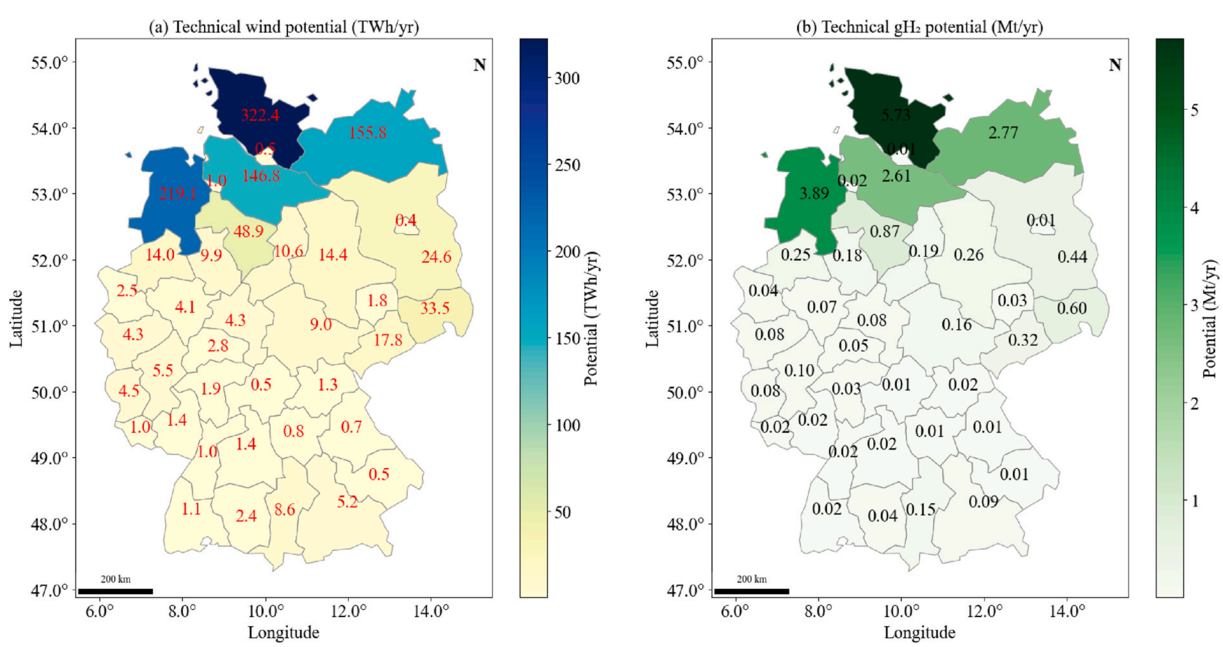

Fig. 7. Final spatially constrained technical onshore wind-to-hydrogen potential after all spatial and terrain constraints. (a) Technical onshore wind energy potential (TWh/year). (b) Technical gH2 potential (Mt/year) assuming 70% electrolyzer efficiency. Results are shown at NUTS-2; electrolyze inputs use the fixed technical parameter set described in the text.

constrained technical gH_2 potential is about 19.3 Mt/year (Fig. 7). Regional disparities are pronounced with northern Germany dominating supply. Schleswig-Holstein alone supporting about 5.7 Mt/year, Lower Saxony 3 to 5 Mt/year, and Mecklenburg-Vorpommern about 2.7 Mt/year. Eastern states such as Brandenburg (about 0.44 Mt/year) and Saxony-Anhalt (about 0.3 Mt/year) are more constrained. Most southern and western regions contribute only 0.02 to 0.15 Mt/year due to terrain constraint, population density, and competing land uses. The 19.3 Mt figure is a technical upper bound, and realized output will be lower because a significant share of wind must remain allocated to electricity demand.

3.2. Stochastic model results

The deterministic baseline provides an upper bound under fixed parameter assumptions, while the stochastic model incorporates uncertainty to generate probabilistic estimates. These estimates capture variability in wind resource availability and key technical parameters, providing a more robust characterization of wind-to-hydrogen potential.

3.2.1. Wind-to-hydrogen potential and uncertainty

Monte Carlo simulations (10,000 samples) yield a slightly right-skewed distribution with a median value of 10.8 Mt/year and mean value of about 10.9 Mt/year (Fig. 8a). The probability of exceeding 8.9 Mt/year is 90%, while the probability of exceeding 13.17 Mt/year is 10%. The 95% confidence interval (CI) ranges from 8 to 14.6 Mt/year, indicating moderate uncertainty with an upper tail relevant for infrastructure planning. Regional distributions widen in high-wind areas due to the cubic wind-power relation (Equation (2)), Schleswig-Holstein (DEF0) and Weser-Ems (DE94) show broader, right-shifted distributions, with means of about 3.35 and 2.28 Mt/year and standard deviations of 1.19 and 0.83 Mt/year, respectively, compared with Lüneburg (DE93: about 1.53 ± 0.60 Mt/year) and Mecklenburg-Vorpommern (DE80: about 1.61 ± 0.58 Mt/year) (Fig. 8b).

3.2.2. Plant sizing optimization and LCoH

Wind and electrolyzer capacities are co-optimized under temporal-matching constraints, yielding regional LCoH distributions. Results assume a base case discount rate of 6%, electrolyzer CAPEX 2500 €/kW and onshore wind CAPEX 1300 €/kW.

Duration-curve LP validation results show that optimal wind and electrolyzer capacities, wind-to-electrolyzer ratios, and LCoH values are indistinguishable within numerical tolerance, confirming that duration-curve compression adequately represents temporal matching for the wind-electrolyzer system considered here. Fig. 9 illustrates the LCoH distributions across 100 weather scenarios for three representative NUTS-2 regions spanning the range of LCoH magnitudes observed across Germany.

Median LCoH spans 7.64 to 18.54 €/kg across NUTS-2 regions (Fig. 10). Lowest medians occur in wind-rich northern and coastal areas, including Schleswig-Holstein (DEF0) 7.64 €/kg, Mecklenburg-Vorpommern (DE80) 7.99 €/kg, Weser-Ems in Lower Saxony (DE94) 8.14 €/kg, Lüneburg in Lower Saxony (DE93) 8.60 €/kg, and Brandenburg (DE40) 9.34 €/kg. Highest values occur inland and in southern Germany, notably Oberbayern, Bavaria (DE21) 18.54 €/kg, Freiburg, Baden-Württemberg (DE13) 17.77 €/kg, Schwaben, Bavaria (DE27) 14.57 €/kg, and Tübingen, Baden-Württemberg (DE14) 14.27 €/kg.

Uncertainty remains comparatively small in low-cost regions and increases substantially in high-cost regions. For example, Schleswig-Holstein (DEF0) shows a relatively narrow interquartile range of 7.29 - 8.10 €/kg, whereas Oberbayern (DE21) exhibits a much wider range of 16.90 - 20.46 €/kg, indicating stronger sensitivity to resource variability in wind-scarce areas.

Capacity patterns are consistent with the cost gradient: median wind-to-electrolyzer overbuild ratios (w/E) remain moderate in low-cost regions, typically around 1.9 - 2.2 (e.g., DEF0 1.88; DE94 2.01; DE93 2.16), and increase to approximately 3.0 - 3.9 in high-cost regions (e.g., DE13 3.48; DE21 3.87). Overall, the merit order is dominated by northern and coastal regions combining low costs with moderate overbuild requirements, while costs rise steeply when moving toward wind-scarce inland and southern regions requiring substantially larger overbuild.

These results indicate that full-load hours (FLH) are the dominant cost driver. Higher FLHs allow the electrolyzer to operate closer to nameplate, limit the wind-to-electrolyzer overbuild ratio (w/E) and reduce capital intensity per kg of H_2. In wind-scarce regions, meeting the same H_2 demand requires disproportionately larger wind capacity, which lowers asset utilization and raises LCoH. Limited space in small and densely populated southern NUTS-2 regions further constrains overbuilding and compounds costs. Thus, competitiveness is governed jointly by resource quality and spatial feasibility, favoring the large northern and coastal regions.

Sensitivity analysis of electrolyzer CAPEX and discount rates reveals the trade-off between capital intensity and financing costs in determining the LCoH is illustrated in Fig. 11.

Fig. 11 demonstrates that LCoH is sensitive to both electrolyzer CAPEX and project discount rate (r), with the latter exerting the dominant influence. At a CAPEX of 2000 €/kW and 2% discount rate, mean LCoH ranges from 5.57 €/kg (DEF0) to 6.28 €/kg (DE93). Increasing the discount rate to 10% raises mean LCoH by approximately 50%, while

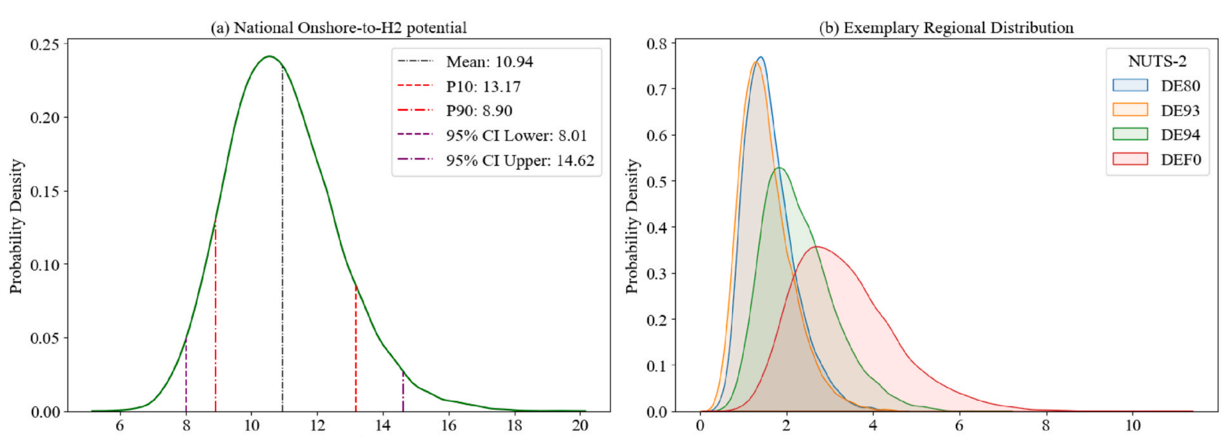

Fig. 8. Probabilistic wind-to-hydrogen spatially constrained technical potential. (a) National distribution from 10,000 Monte Carlo samples (Mt/year). (b) Regional distributions for selected NUTS-2 regions illustrating higher means and wider dispersion in wind-rich areas. The annotations indicate exceedance probabilities, where P10 and P90 denote the values exceeded by 10% and 90% of samples, respectively (i.e., P10 corresponds to the 90th percentile and P90 to the 10th percentile).

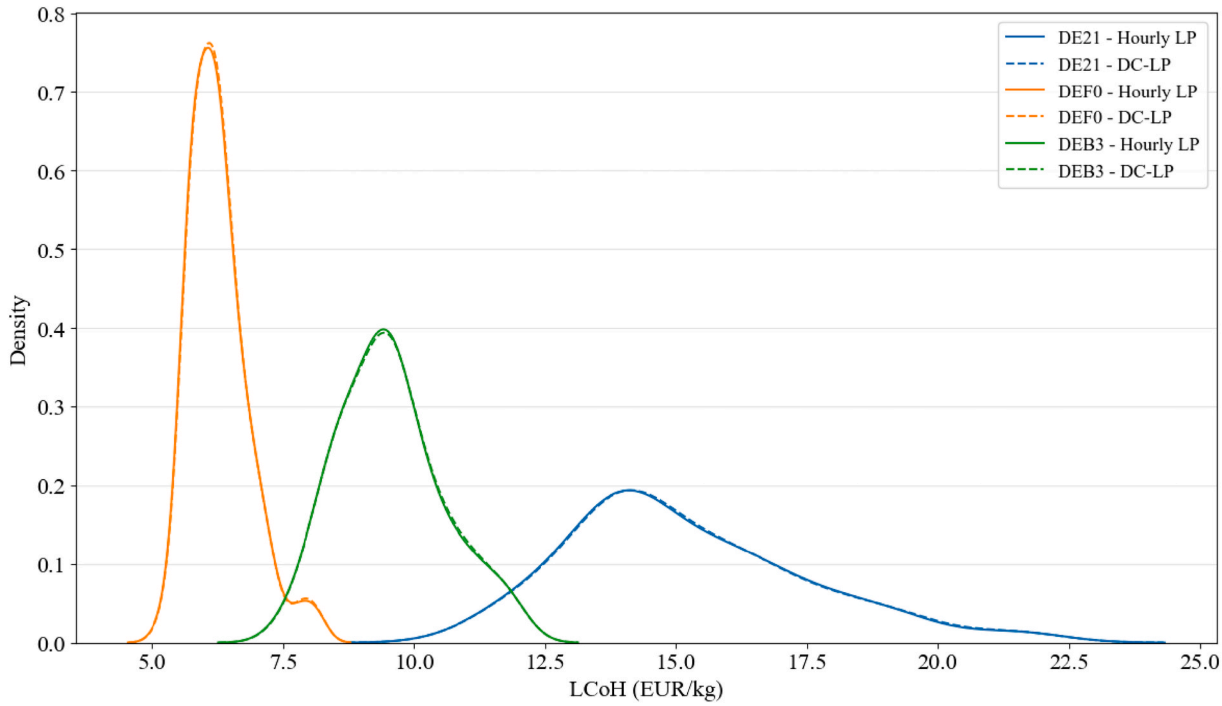

Fig. 9. LCoH distributions from hourly LP (solid lines) and duration-curve LP (dashed lines) for three representative NUTS-2 regions across 100 weather scenarios, illustrating low, mid, and high LCoH regimes.

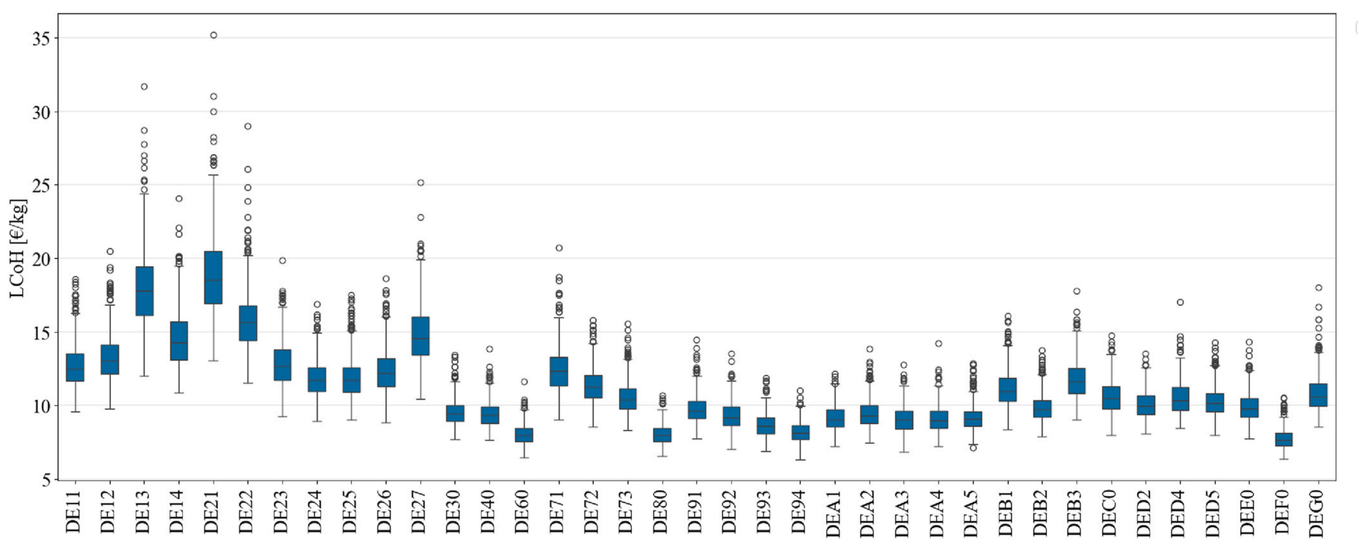

Fig. 10. LCoH distribution across NUTS-2 regions. Median, P05 to P90, and outliers from 500 hourly Monte Carlo simulations per region (each sample is a 20-year profile). Results assume electrolyzer CAPEX of 2500 €/kW and a 6% discount rate.

increasing CAPEX from 2000 €/kW to 2750 €/kW at fixed discount rate contributes a more modest 16 - 18% increase, confirming that financing conditions are a stronger cost driver than capital expenditure within the ranges examined.

A consistent regional ordering is observed across all scenarios, with DEF0 yielding the lowest LCoH and DE93 the highest, with a persistent spread of 0.40 - 0.75 €/kg between them. Parametric uncertainty, reflected in the standard deviation, increases with both higher CAPEX and discount rates, ranging from 0.49 to 1.01 €/kg across all scenarios. Under current private financing conditions (6 - 8% discount rate), mean LCoH across all regions rises to 6.85 - 9.39 €/kg, highlighting the importance of public financing mechanisms in achieving cost-competitive green hydrogen production.

3.2.3. *Wind-to-hydrogen supply curve*

Aggregating regional volumes and costs yields a national supply curve that reveals the merit order and the concentration of low-cost supply. Fig. 12 orders NUTS-2 regions by median LCoH. Box width indicates median annual gH_2 potential, the vertical span shows P05 – P90 LCoH, and the central tick marks the median.

The majority of domestic gH_2 supply on the left-hand side of the merit order is concentrated in a small number of northern and coastal NUTS-2 regions. Schleswig-Holstein (DEF0), Mecklenburg-Vorpommern (DE80), Weser-Ems in Lower Saxony (DE94), and Lüneburg in Lower Saxony (DE93) dominate low-cost volumes, together accounting for roughly 8.3 Mt/year, with Schleswig-Holstein alone contributing about 3.18 Mt/year. Hamburg (DE60) also appears early in the merit order but

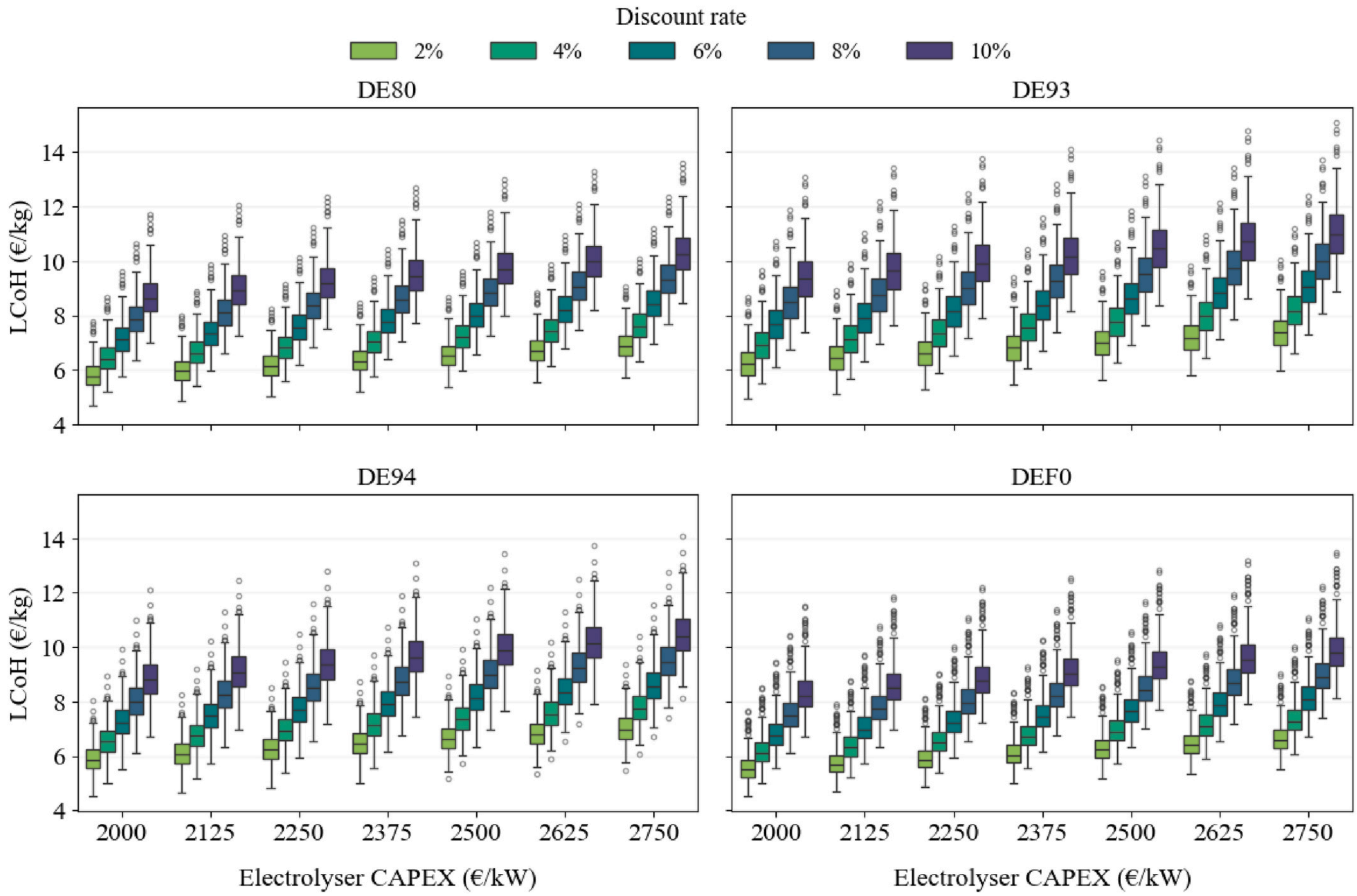

Fig. 11. Sensitivity of the levelized cost of hydrogen (LCoH, €/kg) to electrolyzer CAPEX (€/kW) and discount rate (2% - 10%) across selective NUTS regions (DE80, DE93, DE94, DEF0). Boxplots summarize 500 Monte-Carlo runs per scenario. In all regions, LCoH increases monotonically with both parameters.

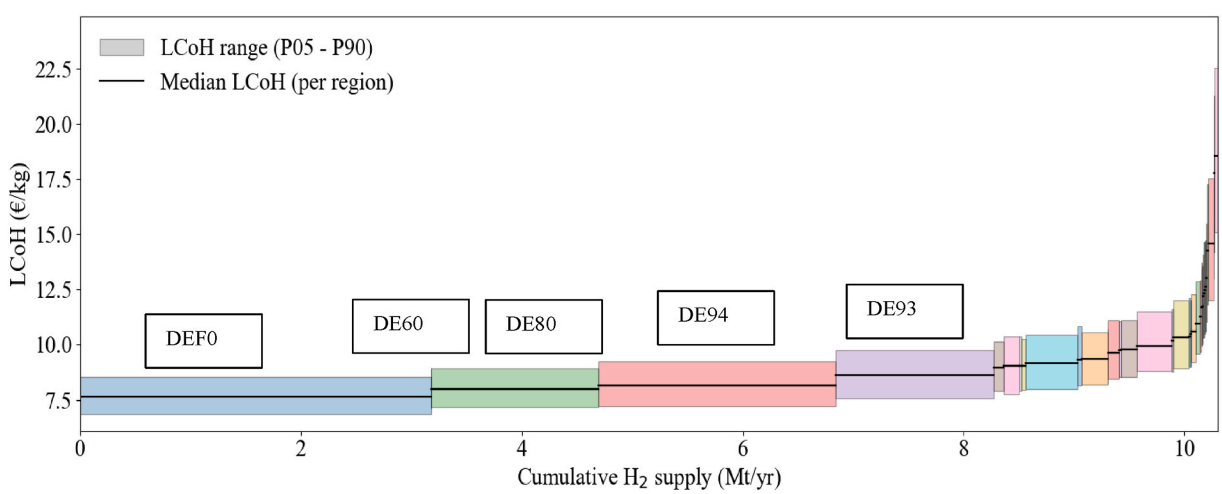

Fig. 12. National wind-to-hydrogen supply curve. Regions are ordered by median LCoH; box width indicates median volume (Mt/year); vertical span shows P05 to P90 LCoH; and the horizontal tick marks the median LCoH. The curve highlights the concentration of low-cost volumes in northern and coastal regions.

contributes only a small additional volume (~0.005 Mt/year). Most other regions enter later with substantially smaller increments at higher LCoH. Median LCoH varies from about 7.64 €/kg in Schleswig-Holstein (DEF0) to about 18.54 €/kg in Oberbayern (DE21). The supply curve is convex, with a large low-cost block from northern and coastal regions followed by steep cost escalation once these regions are exhausted and supply shifts toward inland and southern regions. Uncertainty bands (P05 – P90) are generally moderate, typically around ±0.8 - 1.5 €/kg in low-cost regions (e.g., DEF0 6.88 - 8.53 €/kg, DE94 7.20 - 9.23 €/kg, DE93 7.56 - 9.74 €/kg) and widening in high-cost regions (e.g., DE21 15.07 - 22.53 €/kg, DE13 14.18 - 21.28 €/kg), reflecting greater sensitivity to resource fluctuations in wind-scarce areas. Despite these differences in variability, the overall ordering of regions remains stable, with northern and coastal hubs consistently supplying the majority of low-cost domestic hydrogen volumes.

3.2.4. Sensitivity scenarios: technology and siting effects on gH_2 supply

Fig. 13 examines two design levers for wind-to-hydrogen systems, efficiency gains and turbine spacing, to quantify their impact on gH_2 output and uncertainty. The “Efficient Technology” scenario includes 606 samples where WTG efficiency, electrolyzer efficiency, and availability exceed their 75th percentiles. This subset yields average gH_2 outputs 10.9 Mt/year (range 6.7 to 17.7 Mt/year). Electrolyzer efficiency averages 75.6% (standard deviation 0.25%), while WTG availability averages 90.2%. The “Strict or High WTG spacing” scenario includes 2453 samples where WTG spacing exceeds the 75th percentile. Wider turbine separation lowers land-use intensity but reduces output. Average gH_2 production is 10.31 Mt/year (range 5.96 to 16.76 Mt/year), with 75% of outcomes at or below 11.26 Mt/year. Mean WTG spacing reaches 7.55 rotor diameters, compared to 7.35 in the full sample. These results show that both technology performance and spatial layout influence hydrogen output and uncertainty.

3.2.5. Hydrogen production and demand: spatial distribution

The spatially constrained technical results are placed against indicative supply and demand locations and the planned hydrogen backbone. Project entries from the national registry [47] are harmonized, classified as injection or offtake, and aggregated to state-level net balances. A pronounced north-south divide emerges. Net surpluses concentrate in northern and coastal states. For example, Lower Saxony (15.8 kt/day), Mecklenburg-Vorpommern (8.3 kt/day), Schleswig-Holstein (2.5 kt/day), and Bremen (1.2 kt/day), with Bavaria (3.6 kt/day) and Saarland (4.1 kt/day) acting as secondary exporters. Major deficits occur in demand-intensive regions. For example, North Rhine-Westphalia (−8.3 kt/day), Baden-Württemberg (−4.8 kt/day), Berlin (−3.5 kt/day), Saxony (−3.1 kt/day), and Rhineland-Palatinate (−2.9 kt/day).

This spatial imbalance implies a strong reliance on long-distance north-to-south transmission from northern production hubs to southern demand centers. Balancing regional surpluses and deficits depends on the capacity of inter-state transmission corridors. Fig. 14 overlays the hydrogen core network and highlights the persistent supply-demand mismatch with export potential anchored in wind-rich northern states versus inland industrial demand.

The analysis of Germany's hydrogen backbone indicates most capacity is planned for commissioning by the 2030s [46], with minor reinforcements appearing by 2040. The backbone is denser in the west and north and more fragmented in the east and south. High-capacity links include Darmstadt-Rheinhessen-Pfalz (27.4 kt/day), Brandenburg-Saxony-Anhalt (15.2 kt/day), Brandenburg-Dresden (12.2 to 15.2 kt/day), and Düsseldorf-Münster (18.3 kt/day). Numerous links fall in the 3 to 6 kt/day range, while connections such as Lüneburg-Schleswig-Holstein (2.6 kt/day) and Bremen-Braunschweig (2.4 kt/day) represent the lower end. Although the backbone can support substantial interregional trade, bottlenecks may persist at the periphery and in wind-scarce areas, reinforcing the importance of corridor routing and regionally coordinated siting.

Low-cost, high-volume northern hubs such as Schleswig-Holstein (DEF0, about 3.2 Mt/year at about 7.6 €/kg), Weser-Ems, Lower Saxony (DE94, about 2.1 Mt/year at about 8.14 €/kg), and Lüneburg, Lower Saxony (DE93, about 1.4 Mt/year at about 8.6 €/kg), dominate production, and connect to >12 kt/day backbone corridors, enabling large exports. In contrast, demand concentrates inland industrial and metropolitan regions (i.e., Rhine-Ruhr (DEA1, DEA2), Arnsberg (DEA5), south Stuttgart (DE11), Karlsruhe (DE12), and Freiburg (DE13), where local production remains limited and relatively more expensive. For example, Stuttgart, Karlsruhe, and Freiburg produce <0.01 Mt/year with median cost exceeding 12.40 €/kg. This spatial mismatch implies long-term reliance on transmission from coastal production hubs.

Benchmarking regional outputs against corridor ratings suggests that transmission adequacy may constrain inland supply over the long term. The combined exports of the northern hubs (DEF0, DE94, DE93), totaling over 8 Mt/year, must traverse inland links typically rated between 3 and 12 kt/day (approximately 1.1 to 4.4 Mt/year). Individual regions often fit within adjacent corridor limits, but simultaneous exports from several coastal hubs would saturate these links. In contrast, smaller producers such as Brandenburg (DE40, ~0.24 Mt/year) and Mecklenburg-Vorpommern (DE80, ~1.52 Mt/year) remain below corridor thresholds, suggesting an easier integration into the hydrogen grid.

3.2.6. Hydrogen demand scenario analysis

The spatially constrained technical potential results are compared against demand trajectories and indicative electricity allocation for electrolysis derived from system-level considerations. To justify realistic allocation levels, projected electrolysis electricity demand and onshore

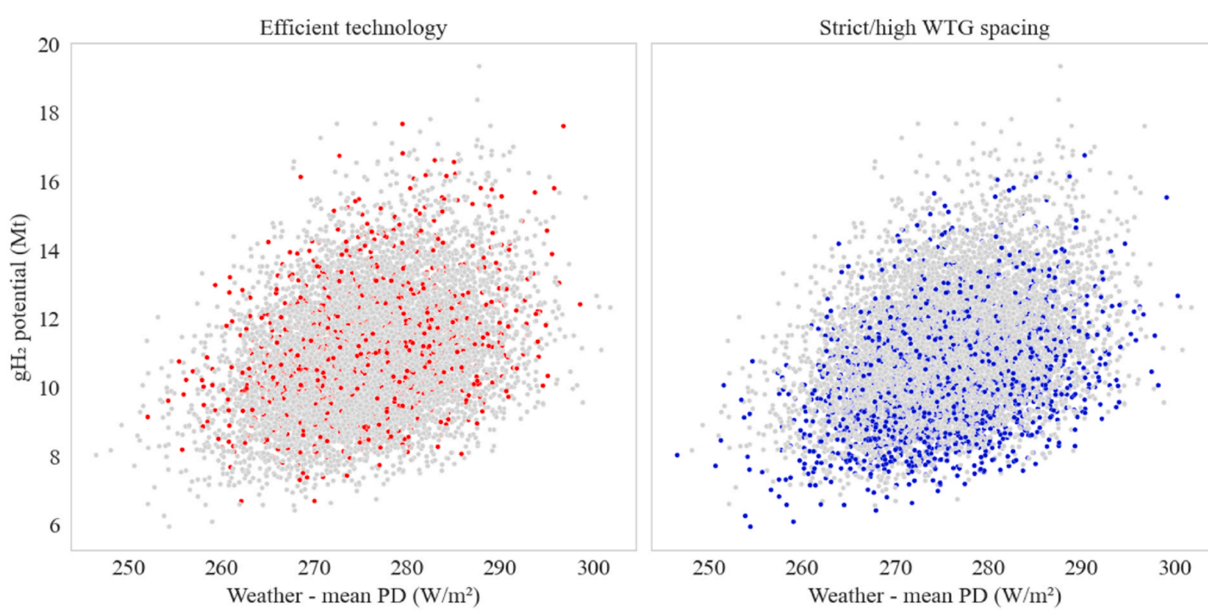

Fig. 13. Scenario slices within the stochastic ensemble. (a) Efficient Technology: samples above the 75th percentile for WTG efficiency, electrolyzer efficiency and availability. (b) Strict or high turbine spacing: samples above the 75th percentile for spacing.

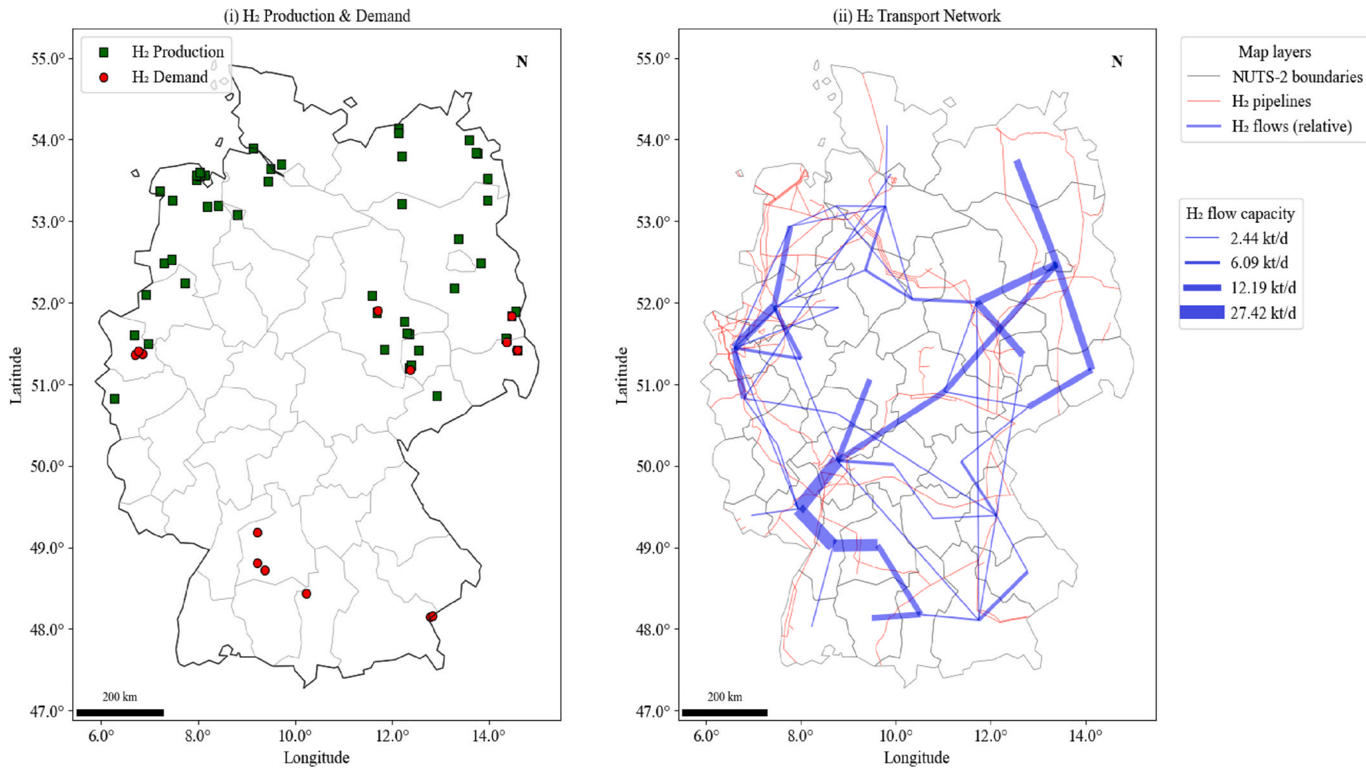

Fig. 14. Production, demand and transport network. (a) State-level hydrogen production and demand locations and net balances. (b) Planned hydrogen transport network; line widths represent aggregated corridor capacities (kt per day) between regional hubs.

wind generation from German 2045 energy system studies are compared (Table 5). The ratio of electrolysis electricity demand to onshore wind generation provides an empirical benchmark for feasible allocation shares.

Across the reviewed studies, implied allocation shares range from approximately 30% to 77%. Values approaching or exceeding 100% occur only in scenarios with very high electrolysis deployment, requiring near-complete dedication of onshore wind generation to hydrogen production. These cases therefore represent upper-bound system conditions rather than typical configurations.

Based on Table 5, the allocation range considered (30 - 100%) represents a structured sensitivity envelope around the technical upper bound. However, a narrower range of 30 - 50% is considered more realistic, with a baseline value of 40% adopted to represent a strongly electrified and integrated energy system. Values above 40% would imply substantial displacement of direct electrification or require large-scale overcapacity, which is not explicitly supported by the studies summarized in Table 5. The 40% value is therefore used as the reference allocation in the interpretation of Fig. 15, while higher shares represent progressively more stringent upper-bound assumptions approaching dedicated wind-to-hydrogen configurations.

Table 5
Implied allocation shares derived from German 2045 electricity system studies based on projected electrolysis electricity demand and onshore wind generation.

Study/Report	Electrolysis Consumption [TWh]	Onshore Wind Production [TWh]	Ratio
Agora [50]	150	509	~30 %
DBI_BCG 2021 [51]	155	440	~35%
BMWK 2024 [52]	240 - 320 Translated From (60 - 80 GW at 4000 FLH)	415	~58 to 77%
NETZ 2025 [53]	273 - 440 Translated From (61 - 110 GW at 4000 FLH)	384 - 431	~64 to 101%

This allocation analysis translates the spatially constrained technical potential into realizable hydrogen supply estimate (i.e., system-constrained), linking resource-based potential to integrated energy system feasibility.

To benchmark against the projected hydrogen demand levels, two scenarios are evaluated: a base case aligned with government wind capacity targets and a spatially constrained technical potential case representing the upper development limit.

The base scenario assumes onshore wind capacity of 64 GW in 2024, 115 GW in 2030, and 160 GW in 2045 [5]. At 70% electrolyzer efficiency and 26.7% historical CF, these capacities correspond to green hydrogen equivalent outputs of approximately 2.66, 4.78, and 6.65 Mt, respectively (i.e., nominal and dedicated hydrogen production). Germany's hydrogen strategy targets at least 10 GW of electrolysis by 2030 [2], implying an annual electricity demand of 35 - 45 TWh at 40 - 50% utilization, equivalent to approximately 0.62 - 0.80 Mt/year of green hydrogen. This represents 5.7 - 7.3% of the national spatially constrained technical potential estimated in this study.

The spatially constrained technical potential scenario assumes accelerated deployment of corresponding wind capacity by 2045, such that total onshore wind generation could support approximately 10.8 Mt/year of hydrogen production (i.e., the median of the spatially constrained technical potential). Only 60% of this capacity is assumed to be installed by 2030, consistent with typical project lead times of 2 - 6 years [54]. Fig. 15 benchmarks these projections against Germany's national hydrogen demand targets of 1.4 Mt in 2024, 2.4 - 3.3 Mt by 2030, and 9.3 - 13.7 Mt by 2045 [2]. The results indicate adequate near-term demand coverage but reveal significant deficits by 2045 under lower electricity allocation scenarios, underscoring the need for complementary renewable integration, hydrogen imports, or demand-side measures.

Fig. 15 shows a widening gap between onshore wind gH_2 realizable supply and national H_2 projected demand over time, particularly under

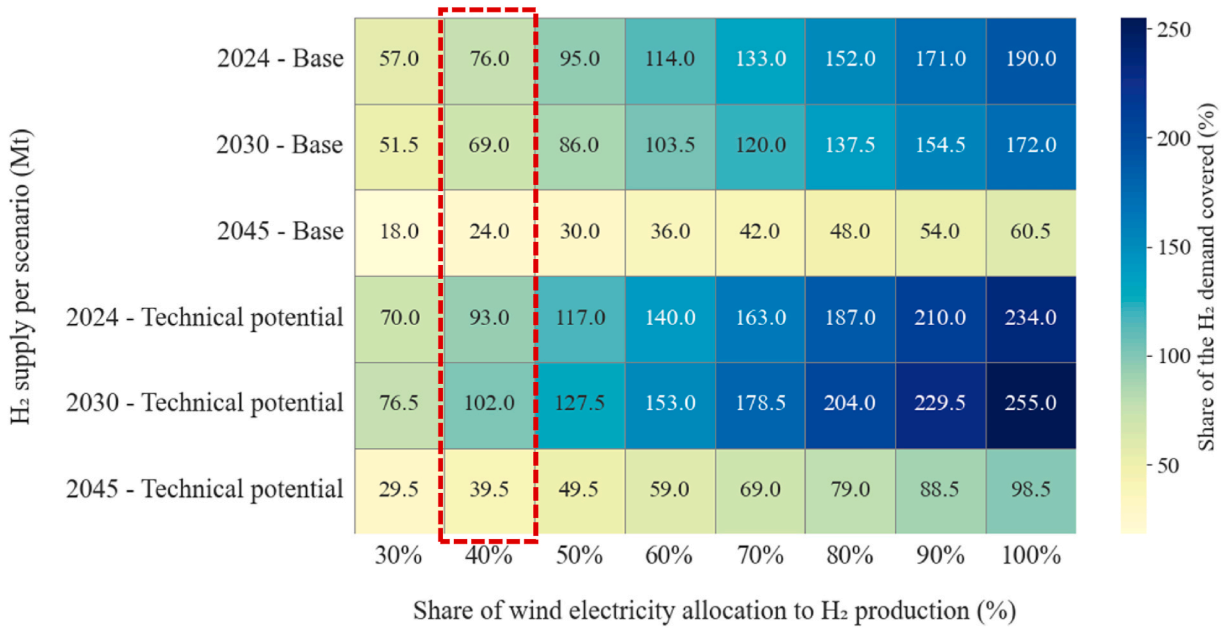

Fig. 15. Coverage of national hydrogen demand by onshore-wind-based gH_2 under capacity and allocation assumptions. Rows indicate year and supply capacity case (Base: 64 GW in 2024, 115 GW in 2030, 160 GW in 2045; Technical potential: probabilistic technical limit with 60% realization by 2030 and full by 2045). Columns show the share of onshore wind electricity allocated to electrolysis (30 to 100%). Each cell reports the share of national hydrogen demand covered (average % of the demand range) using central demand estimates (1.4 Mt in 2024, 2.4 - 3.3 Mt in 2030, 9.3 - 13.7 Mt in 2045), assuming 70% electrolyzer efficiency and a historical 26.7% capacity factor for onshore wind energy. Values above 100% indicate surplus relative to demand. Only onshore wind is considered.

the base scenario. In 2024, existing capacity can meet demand even with moderate electricity allocation (50 - 60%). By 2030, full coverage under the base case requires allocations of at least 60%. By 2045, the base case falls short even at 100% allocation, covering about 49 - 72% (mean of 60.5%) of projected demand.

The technical potential scenario indicates that demand in 2030 can be fully met at allocation shares of approximately 40% or higher. By 2045, allocating 30 - 50% of onshore wind generation to electrolysis constrains realizable domestic hydrogen supply to approximately 3.2 - 5.4 Mt/year. This corresponds to only 34.8 - 58.1% of the lower demand estimate and 23.6 - 39.4% of the upper demand estimate, indicating a substantial gap. Even the upper bound of the spatially constrained technical potential is insufficient to meet projected demand (can only cover the lower range of demand).

The relationship between electricity allocation and demand coverage is approximately monotonic but differs across scenarios. In the base scenario (2045), increasing allocation from 30% to 100% raises coverage from 18.0% to 60.5%, corresponding to an absolute increase of 42.5 percentage points and a marginal effect of approximately 0.61 percentage points of demand coverage per 1% increase in allocation. In contrast, the spatially constrained technical potential scenario exhibits a near-linear response, with coverage increasing from 29.5% to 98.5% (+69 percentage points), corresponding to a slope close to unity (~0.99). In relative terms, both scenarios show a similar ~3.3-fold increase; however, absolute differences remain decisive for system adequacy. These results indicate that allocation has a strong but structurally constrained effect, particularly in the base scenario where even full allocation remains insufficient to meet demand.

These results demonstrate that electricity allocation is a first-order determinant of realizable hydrogen supply, exceeding the impact of parametric uncertainty in resource and technology assumptions. Consequently, domestic wind-based hydrogen production cannot meet long-term demand without complementary supply sources, across all realistic allocation assumptions.

3.2.7. Uncertainty quantification & sensitivity analysis

Global sensitivity analysis identifies the most influential parameters contributing to uncertainty in gH_2 production. Table 6 summarizes the direct (first-order Sobol indices, S_1) and interaction effects (total-order Sobol indices, S_t) across five parameters. WTG spacing emerges as the dominant driver, explaining approximately 74 to 77% of variance. Weather variability is the second most influential factor. Other parameters such as WTG efficiency, electrolyzer efficiency, and availability, contribute marginally within the assumed ranges (see Table 7).

One-at-a-time perturbations illustrated in Fig. 16 reinforce these findings. Spacing variations cause substantial output spread (standard deviation 4.1 Mt), weather variability introduces notable uncertainty (standard deviation 2 Mt), and other parameters have minimal impact (coefficients of variation <0.08).

Turbine spacing emerges as the dominant uncertainty driver, accounting for the majority of output variance. This contrasts with prior studies (e.g., Attiaoui [10]), which often emphasize weather variability and employ typical meteorological year approaches to reduce inter-annual uncertainty. In the present spatially explicit framework, weather-related variability contributes substantially less to overall variance. This difference reflects the focus of the analysis. For long-term resource potential assessment under spatial constraints, land-use intensity and turbine deployment density exert a stronger influence on aggregate output than inter-annual weather variability. By contrast, for cost and operational performance assessments, where temporal variability and utilization are critical, weather-related uncertainty remains

Table 6
Sobol sensitivity indices (S_1, direct effects; S_t, total effects) for key parameters affecting green hydrogen production.

Parameter	S_1	S_t	Interpretation
Spacing	0.74	0.77	Most influential; spacing alone explains about 74 to 77% of gH_2 variance
Weather variability	0.16	0.19	Significant effect from wind variability
WTG efficiency	0.026	0.03	Small but non-negligible direct effect
Electrolyzer efficiency	0.002	0.009	Small influence
Availability	0.003	0.003	Negligible impact within the given bounds

Table 7
Summary of key modelling factors and their quantified impact relative to the central estimate (Monte Carlo median of 10.8 Mt/year) of the spatially constrained technical potential.

Assumption	Value/ Range	Informed by/ source	Impact on H_2 output
Wind allocation	40%	[50] to [53]	− 60%
Turbine spacing	10D	[34], [35]	− 56% % (10D vs ~7D spacing)
Weather variability	CV 10 - 16%	[23]	±10 to 15%

highly relevant.

These findings indicate that uncertainty prioritization is context-dependent, with spatial planning and land-use constraints playing a central role in resource potential estimation, while weather variability and technology performance remain key drivers in techno-economic and operational analyses. Accordingly, within spatially constrained resource assessments, siting and land-use parameters may be more influential than commonly emphasized sources of uncertainty.

3.2.8. *Quantitative impact of key modelling assumptions*

This section summarizes the impact of key modelling assumptions and quantifies their effect on national hydrogen output and cost distributions. Marginal impacts were estimated using a log-linear regression of Monte Carlo results, in which the logarithm of hydrogen production is regressed against key input parameters, allowing coefficients to be interpreted as approximate semi-elasticities over the sampled parameter ranges. The regression-based estimates are used to support interpretation of marginal effects rather than to replace the variance-based sensitivity framework.

Wind allocation to electrolysis: The technical potential (10.8 Mt/year median) assumes dedicated wind capacity. Introducing system-consistent allocation constraints reduces available electricity. Under a 40% allocation scenario, hydrogen output declines to approximately 4.4 Mt/year (−60%), indicating that allocation assumptions dominate the gap between technical and realizable potential. This confirms that the reported technical potential represents an upper bound rather than a deployable estimate.

Turbine spacing and land-use intensity: Variations in turbine spacing from 5D to 10D directly scale land-use efficiency and therefore the spatially constrained technical potential, resulting in variation in hydrogen output. Increasing turbine spacing from typical values (7D) to wider layouts (10D) reduces hydrogen output by approximately 56% while dense layouts (5D) can increase output by ~70%, reflecting the strong inverse relationship between spacing and capacity density. Consistent with this scaling effect, Sobol analysis identifies spacing as the dominant uncertainty driver, explaining approximately 74 - 77% of total output variance.

Weather variability: Stochastic perturbations capture interannual variability in wind power density (CV ~10 to 16%), resulting in moderate variations in hydrogen output of approximately ±10 to 15%. This reflects the use of aggregated power density as model input, in which the cubic dependence on wind speed is already embedded and temporally averaged, and is consistent with the Sobol sensitivity analysis, which attributes approximately 16 to 19% of total output variance to weather variability.

Overall, these results demonstrate that the main findings are robust across the tested assumptions. Domestic wind-based realizable hydrogen supply is structurally insufficient to meet national demand under system-integrated conditions, turbine spacing strongly influences the estimated spatially constrained technical potential, while weather variability introduces moderate uncertainty in hydrogen output. System-level factors, particularly electricity allocation, primarily determine the magnitude of the supply gap.

4. Discussion

The modelling framework combines high-resolution geospatial resource assessment with probabilistic uncertainty propagation and a reduced-form representation of system consistency. The spatially constrained wind-to-hydrogen potential is derived from physically

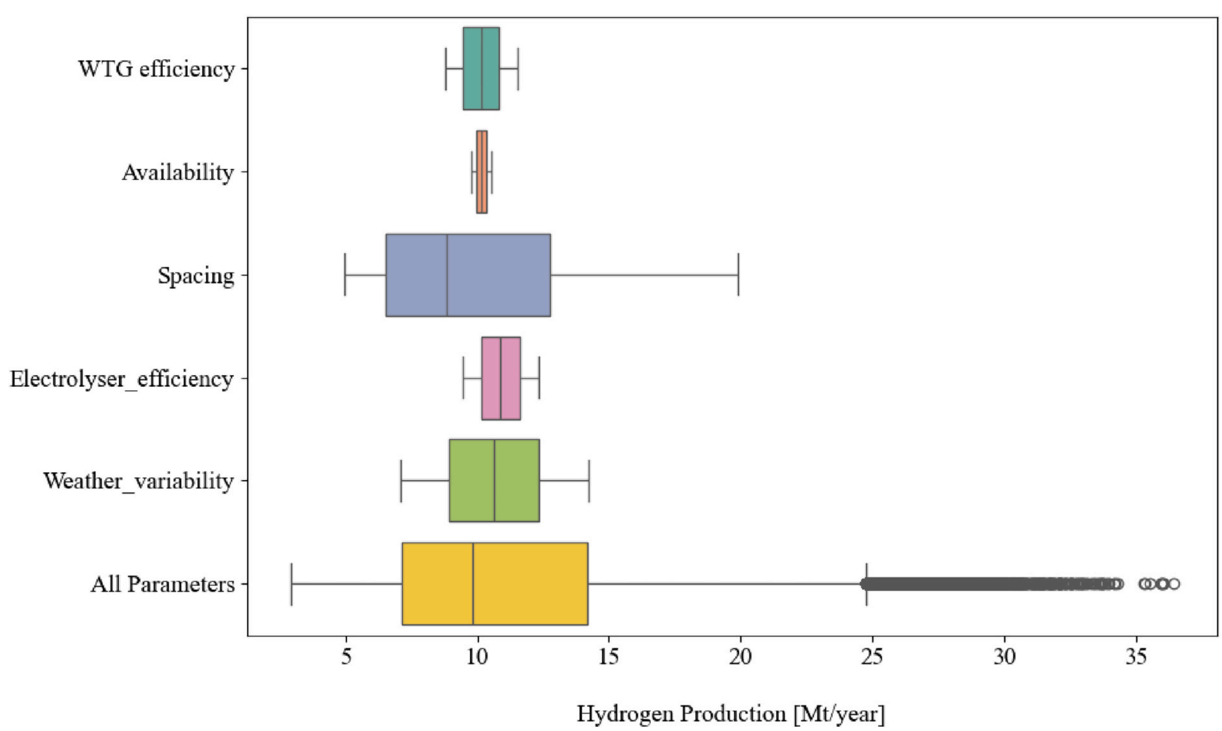

Fig. 16. One-at-a-time parameter perturbations and production variability. Boxplots show distributions of hydrogen production when varying each parameter individually and when varying all parameters simultaneously; spacing and weather dominate variance.

grounded constraints, including land eligibility, turbine spacing, and resource variability, and therefore represents a robust estimate of the maximum technically achievable output under spatial feasibility conditions. The temporal and techno-economic components are designed to ensure internal consistency of wind-electrolyzer coupling rather than to reproduce a full energy system equilibrium.

The linear programming (LP) formulation (Section 3.2.2) enforces renewable-constrained hydrogen production by limiting electrolyzer dispatch to contemporaneous wind availability, providing an RFNBO-consistent representation of temporal coupling. Temporal matching is implemented using duration-curve aggregation rather than explicit hourly chronology. This approximation is justified by the model structure: in the absence of storage, grid exchange, or inter-temporal constraints, system performance depends on the distribution of wind availability rather than its sequence. As a result, duration-curve aggregation preserves the feasible production space and yields equivalent optimal sizing and LCoH under the present assumptions. Accordingly, the framework provides a robust representation of renewable-constrained hydrogen production for resource assessment and cost estimation, but it is not intended as a full system-dispatch or regulatory compliance model. Technical potential estimates remain unaffected by this approximation, as they are derived from aggregated annual energy, while cost results should be interpreted within the assumed system representation.

Additionally, system-level interactions are incorporated through complementary mechanisms rather than full endogenous modelling. In particular, scenario-based allocation of wind generation to electrolysis captures competition with electricity demand, while the static infrastructure benchmarking provides an indicative assessment of spatial mismatches between production and demand centers. These elements extend the analysis beyond pure resource assessment and show that realizable (i.e., system constraint) hydrogen supply is structurally lower than the spatially constrained technical potential. In practice, further system constraints, including grid limitations, temporal balancing requirements, infrastructure availability, and regulatory conditions, would reduce the realizable share of this spatially constrained technical potential. The allocation scenarios presented here provide a first-order indication of this effect, illustrating the transition from a technically upper bound toward realizable supply levels.

Accordingly, this stochastic framework produces a distribution of outcomes rather than a single estimate. The national spatially constrained technical potential centers on a median of about 10.8 Mt/year, with a P05 – P95 range of roughly 8 - 14.6 Mt/year, and rare tails below 6 Mt/year or above 19 Mt/year. Infrastructure and system planning should therefore rely on quantile-based benchmarks. The P05 estimate provides a conservative supply floor, the P50 represents the baseline planning case, and the P95 indicates upper-bound optionality for infrastructure sizing. Planning within these probabilistic bands reduces the risk of systematic over- or under-investment relative to deterministic mean estimates. Upper-tail outcomes remain conditional on land availability, permitting, and transport corridor capacity under RFNBO constraints.

Spatially, technical supply potentials are highly concentrated in a small number (4) of northern and coastal NUTS-2 regions, including Schleswig-Holstein (DEF0), Weser-Ems (DE94), Lüneburg (DE93), and Mecklenburg-Vorpommern (DE80), which together exceed 8 Mt/year of spatially constrained technical potential. In contrast, hydrogen demand is concentrated in inland industrial clusters such as the Rhine-Ruhr region and southern metropolitan regions, where local production potential is limited. This spatial mismatch indicates that hydrogen transport infrastructure is likely to be critical for efficient utilization of spatially concentrated supply. Even when sufficient renewable production potential exists in northern regions, the utilization of these volumes depends on the ability of pipeline corridors to deliver hydrogen to inland demand hubs.

The uncertainty analysis further identifies turbine spacing as the dominant driver, explaining approximately 74 - 77% of the variance in hydrogen output, followed by weather variability. Scenario analysis confirms actionable design levers. High-efficiency “best-available technology” configurations increase output, while wider turbine spacing substantially reduces production. These findings highlight land-use layout and spatial planning as first-order determinants of wind-to-hydrogen potential. Technological improvements such as larger rotors, taller hub heights, and higher specific yields can incrementally increase generation and reduce LCoH. However, large increases in onshore wind-based hydrogen supply are more likely constrained by land availability, permitting procedures, and social acceptance than by turbine efficiency alone. Future expansion therefore requires integrated system planning that aligns electrolyzer siting with land-use policy, biodiversity protection, and incentive mechanisms for additional RFNBO-compliant renewable capacity.

Onshore wind alone is unlikely to meet Germany's long-term hydrogen demand. The spatially constrained technical potential, with a central estimate of approximately 10.8 Mt/year, is of similar magnitude to projected demand (9.3 - 13.7 Mt/year by 2045), but does not account for competing electricity uses. When these are considered through scenario-based allocation, the realizable domestic supply declines substantially. Under realistic allocation ranges (30 - 50%), realizable domestic hydrogen supply declines to approximately 3.2 - 5.4 Mt/year. Under an assumption that 40% of onshore wind generation is available for electrolysis, realizable hydrogen production is approximately 4.3 Mt/year, corresponding to about 32 - 46% of projected demand. This gap suggests that additional supply from other renewable sources (e.g., offshore wind and utility-scale PV) and imports will likely be required.

Under the base-case assumptions, regional LCoH ranges from 7.6 to 18.4 €/kg, with electrolyzer full-load hours (FLH) emerging as the dominant cost driver. High-FLH regions operate electrolyzer close to nameplate capacity, require only moderate wind overbuild (w/E ∼ 1.9 - 2.2), and therefore achieve lower capital intensity per kilogram of hydrogen. In contrast, wind-scarce regions require substantially higher overbuild ratios (w/E ∼3.0 - 3.9), which reduces electrolyzer utilization and increases LCoH. As a result, coastal and northern regions, including Schleswig-Holstein (DEF0), Weser-Ems (DE94), Lüneburg (DE93), and Mecklenburg-Vorpommern (DE80), emerge as the most cost-competitive production hubs, consistent with previous studies [16]). Smaller or densely populated southern NUTS-2 regions, such as Oberbayern (DE21) and Freiburg (DE13), face tighter spatial constraints that limit turbine installation and restrict the ability to overbuild wind capacity. This creates a structural double disadvantage: higher hydrogen production costs and stronger land-use pressure. These results highlight that regional hydrogen competitiveness depends jointly on wind resource quality and spatial feasibility.

The LCoH sensitivity analysis indicates that financing conditions play a dominant role in determining hydrogen production costs. The LCoH sensitivity analysis in Fig. 11 shows that regional characteristics exert a structural influence that is not offset by moderate variations in CAPEX or discount rates. Across the tested CAPEX range of 2000 - 2750 €/kW, the separation between discount-rate scenarios is consistently larger than the incremental changes associated with CAPEX increases. This indicates that LCoH is more sensitive to financing conditions than to moderate capital cost variations. Higher discount rates also lead to wider interquartile ranges and a greater number of high-cost realizations, reflecting increased cost uncertainty. As a result, financing conditions and regional wind characteristics emerge as the primary levers for cost reduction in dedicated wind-to-hydrogen systems.

The regional median LCoH reported here is calculated for wind-only, dedicated supply, with electrolyzer dispatch constrained to the wind generation profile. A Monte Carlo benchmark for Germany projects long-term onshore wind hydrogen costs of approximately 2.7 - 4.3 €/kg by 2050 [13]. The higher costs observed in this study mainly reflect stricter operational assumptions, particularly the absence of grid balancing, hybridization, or storage. Allowing such flexibility could increase electrolyzer full-load hours and reduce LCoH [42]. The LCoH reported here should therefore be interpreted as a conservative upper bound under dedicated, renewable-constrained operation.

Despite the valuable insights provided, several limitations remain. Weather variability is represented by using regionally aggregated historical wind power-density distributions at the NUTS-2 level. While this approach captures long-term variability, it does not explicitly represent intra-regional spatial correlations or extreme multi-year low-wind events. Consequently, tail risks relevant for infrastructure sizing may be underestimated. The analysis quantifies a spatially constrained technical potential under stylized assumptions: real-world deployment will be further reduced by competing electricity demand, market dynamics, and permitting constraints. Future electricity demand trajectories are not explicitly integrated into the potential assessment. Several further uncertainties, including electrolyzer availability, curtailment, and evolving grid conditions, would narrow feasible supply.

Electrolysis is modelled as an aggregated conversion process with a single efficiency distribution, without distinguishing PEM, alkaline, or high-temperature technologies. Wind CAPEX is held constant throughout. Transmission findings are indicative, derived by comparing modelled nodal flows against published corridor ratings rather than from a fully endogenous network model; the static pipeline assessment likewise omits flow optimization, storage buffering, line-pack effects, and congestion pricing.

Future work could address these gaps by incorporating technology-resolved electrolysis models with differentiated operational constraints and cost structures, extending sensitivity analysis to wind capital costs and supply-chain constraints, and replacing the static pipeline benchmark with a dynamic hydrogen network optimization model encompassing storage, temporal flow dispatch, and endogenous congestion.

Countries with limited land availability but strong wind resources, such as the Netherlands, Denmark, and Japan, face similar trade-offs between renewable potential, spatial constraints, and hydrogen demand. The stochastic-spatial framework developed here provides a transferable method for quantifying these trade-offs under uncertainty. By linking geospatial siting constraints, probabilistic resource variability, and techno-economic performance, the approach enables risk-aware planning of hydrogen production systems. This integrated perspective supports evidence-based decisions on the scale, location, and infrastructure requirements of renewable hydrogen, contributing to more resilient pathways toward national decarbonization goals.

5. Conclusion

This work provides a probabilistic, spatially explicit national map of Germany's onshore wind-to-hydrogen potential by integrating high-resolution geospatial siting constraints with Monte-Carlo uncertainty quantification. By explicitly representing spatial heterogeneity and weather variability, the framework advances beyond deterministic assessments and produces probabilistic estimates of hydrogen supply and cost.

The analysis estimates a central spatially constrained technical potential of approximately 10.8 Mt/year, with a 95% interval of 8 to 14.6 Mt/year and an upper tail approaching 19 Mt/year under favorable assumptions. Compared to deterministic upper-bound estimates, the probabilistic results indicate a reduction of approximately 44% when uncertainty in resource and technical parameters is explicitly accounted for. Under scenario-based allocation where 40% of onshore wind generation is available for electrolysis, the realizable domestic hydrogen supply (4.3 Mt/year) corresponds to approximately 32 - 46% of projected 2045 demand (9.3 - 13.7 Mt/year), suggesting a structural supply gap if relying on onshore wind alone. EU additionality requirements constrain hydrogen production to newly deployed renewable capacity, reinforcing the dependence of realizable supply on the scale and timing of future renewable expansion.

The results indicate pronounced regional asymmetries in hydrogen competitiveness. Electrolyzer utilization (full-load hours), determined by wind resource quality and the wind-to-electrolyzer ratio (w/E), is identified as the primary cost driver. Northern and coastal regions achieve LCoH values of approximately 7.6 - 8.6 €/kg with moderate overbuild (w/E $\sim$2), whereas inland and southern regions require higher overbuild (w/E $\sim$3 - 4) and exhibit costs of approximately 14 - 18 €/kg. LCoH is found to be more sensitive to full-load hours and financing conditions than to electrolyzer CAPEX, highlighting the dominant role of resource quality and cost of capital in determining economic performance.

As a result, low-cost hydrogen supply is geographically concentrated in northern Germany, implying increasing reliance on transport infrastructure to connect production hubs with inland demand centers. This spatial concentration underscores the need for coordinated corridor development and siting strategies, as transport constraints may limit the effective delivery of low-cost hydrogen.

Turbine spacing and wind variability are identified as the dominant contributors to output uncertainty, indicating that spatial design parameters exert a stronger influence on system outcomes than electrolyzer performance within the examined parameter ranges.

The findings suggest that meeting Germany's long-term hydrogen targets will require a diversified renewable portfolio combining onshore wind, offshore wind, large-scale photovoltaics, and cross-border renewable imports, supported by coordinated infrastructure planning and regulatory clarity for RFNBO-compliant hydrogen production. The probabilistic framework developed here provides risk-aware bounds, rather than single point estimates, to inform strategic decisions on the scale, location, and sequencing of renewable hydrogen development.

These results should be interpreted within the scope of the modelling assumptions. The analysis focuses on spatial and techno-economic feasibility and does not explicitly represent permitting timelines, detailed electricity system dynamics, or endogenous hydrogen network operation. While the estimates represent a technical upper bound on domestic wind-to-hydrogen potential, realizable supply will depend on renewable capacity expansion, allocation to electrolysis, infrastructure development, regulatory frameworks (e.g., RFNBO requirements), and integration with the broader energy system.

Overall, these results emphasize that the scalability of domestic wind-based hydrogen in Germany is governed not only by resource availability, but also by spatial constraints and system-level integration factors.

Declaration of generative AI and AI-assisted technologies

During the preparation of this work, the author used ChatGPT (OpenAI) to optimize portions of the code used in the analysis and to check the clarity and coherence of some sentences. After using this tool, the author reviewed and edited all generated content as needed and takes full responsibility for the content of the published article.

CRediT authorship contribution statement

Munzer Osman: Conceptualization, Data curation, Formal analysis, Investigation, Methodology, Project administration, Resources, Software, Validation, Visualization, Writing – original draft. **Maria Mercedes Movsessian:** Conceptualization, Investigation, Project administration, Supervision, Validation, Writing – review & editing.

Declaration of competing interest

The authors declare that they have no known competing financial interests or personal relationships that could have appeared to influence the work reported in this paper.

Abbreviations

Abbreviation	Definition
ALK	Alkaline Electrolyzer
CI	Confidence Interval
CV	Coefficient of Variation
CF	Capacity factor
DA	Delegated Act
FLH	Full-Load Hours
GIS	Geographic Information System
gH_2	Green Hydrogen
GW	Gigawatt
MWh	Megawatt hour
IRENA	International Renewable Energy Agency
LP	Linear Programming
MC	Monte Carlo
MCDA	Multi-Criteria Decision Analysis
Mt	Million Tons
Kt/d	Kilotons per day
kg	Kilogram
MW	Megawatt
NUTS	Nomenclature of Territorial Units for Statistics
PEM	Proton Exchange Membrane
PtX	Power-to-X
QMC	Quasi-Monte Carlo
RED III	Renewable Energy Directive III
RFNBO	Renewable Fuels of Non-Biological Origin
WTG	Wind Turbine Generator
EU	European Union
PyPSA	Python for Power System Analysis
DOE	Department of Energy
S_1	Sobol first-order effect
S_t	Sobol total-order effect
PDF	Probability Density Function
€	Euros
HHV	Higher heating value
GWA	Global wind atlas
FLH	Full load hours
ERA5	ECMWF Reanalysis - fifth generation
BNetzA	Bundesnetzagentur (Federal Network Agency)

Nomenclature

Symbol	Description	Unit
$\boldsymbol{v}$	Wind Speed	m/s
$\boldsymbol{A}$	Weibull scale parameter	-
$\boldsymbol{k}$	Weibull shape parameter	-
$\boldsymbol{epx}$	Exponential function	-
C	Cost	€
C_e	Electricity cost	€/MWh
$\boldsymbol{PD}$	Power density	watt/m^2
$\boldsymbol{\rho}$	Air density	Kg/m^2
D	WTG rotor diameter	m
$\boldsymbol{\eta_{Betz}}$	Betz limit	%
$\boldsymbol{\eta_{sys}}$	WTG system conversion losses	%
$\boldsymbol{P_e}$	Extractable wind power	watt
$\boldsymbol{P_o}$	Operational power	watt
$\boldsymbol{P_t}$	Technical power	watt
$\boldsymbol{f_{util}}$	Land use utilization	-
$\boldsymbol{\varphi}$	WTG center to center spacing	m
$\boldsymbol{M_l}$	Land cover mask	-
$\boldsymbol{M_p}$	Protected area mask	-
$\boldsymbol{M_e}$	Elevation mask	-
$\boldsymbol{M_s}$	Slope mask	-
$(\boldsymbol{x}, \boldsymbol{y})$	WTG coordinates	-
$\boldsymbol{Prod_{total}}$	Total technical potential of wind energy	GWh
$\boldsymbol{Prod_{gH2}}$	Total technical potential of hydrogen	Mt
E [ ]	Expected value	-
$\boldsymbol{\theta_{pert,i}}$	The perturbed scale	-
$\boldsymbol{\epsilon_i}$	Multiplicative perturbation factor	-
Γ	Gamma function	-

(continued on next page)

(*continued*)

Symbol	Description	Unit
F_{Γ}^{-1}	Quantile function of the gamma distribution	-
LCoH	Levelized cost of hydrogen	€/kg
CAPEX	Capital Expenditure	€
OPEX	Operating expenditure	€/year
C_E	Electrolyzer capital costs	€
C_w	Wind farm capital costs	€
O_E	Electrolyzer operational costs	€/year
O_w	Wind farm operational costs	€/year
E	Electrolyzer nominal capacity	MW
w	Wind farm nominal capacity	MW
w/E	Wind-to-Electrolyzer Capacity Ratio	-
DF_{10}	10 years discount factor	-
ψ	Electrolyzer mid-life replacement fraction	-
r	Discount rate	%
t	Time	year
g	OPEX escalation rate	%/year
μ	Mean value	-
σ	Standard deviation	-
η	Electrolyzer efficiency	%
k	Wind to Electrolyzer ratio	-
$p_{t,b}$	Electrolyzer dispatch in year t, bin b	MW
$\bar{a}$	Wind availability	-

Data availability

All datasets, model scripts and code used for this study are publicly available and can be accessed at [GitHub].

References

[1] Weißenburger B, Wietschel M, Lux B, Rehfeldt M. The long term price elastic demand of hydrogen – a multi-model analysis for Germany. Energy Strategy Rev 2024;54. https://doi.org/10.1016/j.esr.2024.101432.

[2] Federal Ministry for Economic Affairs and Climate Action (BMWK). National hydrogen strategy Update-. 2023. https://www.bundeswirtschaftsministerium.de/Redaktion/EN/Publikationen/Energie/national-hydrogen-strategy-update.pdf?__blob=publicationFile.

[3] Wietschel M, Riemer M, Thomann J, Ragwitz Ombeni Ranzmeyer M, Voglstätter C, Mendler F, Holst M, Hank C, Stamm A, Strohmaier Zarah Thiel R, Müller M, Löschel Ruhr A, Wietschel Martin Wietschel M. HYPAT final report. Karlsruhe: Fraunhofer ISI; 2024. https://hypat.de/hypat-wAssets/docs/new/publications/HYPAT-Final-report.pdf.

[4] Peterssen F, Schlemminger M, Lohr C, Niepelt R, Bensmann A, Hanke-Rauschenbach R, Brendel R. Hydrogen supply scenarios for a climate neutral energy system in Germany. Int J Hydrogen Energy 2022;47:13515–23. https://doi.org/10.1016/j.ijhydene.2022.02.098.

[5] Federal Network Agency, Bundesnetzagentur. Statistics on electricity generation capacity of selected renewable energy sources. Marktstammdatenregister (MaStR) August 2025 , p. 1-2 , table.2. https://www.marktstammdatenregister.de/MaStR/.

[6] Backwell B, Clarke E. GWEC, global wind report -. https://26973329.fs1.hubspotusercontent-eu1.net/hubfs/26973329/2.%20Reports/Global%20Wind%20Report/GWEC%20Global%20Wind%20Report%202025.pdf?_hstc=45859835.097739f84d7d5527f6771afbfde39935.1745426990438.1745426990438.1745426990438.1&_hssc=45859835.2.1745426990439&_hsfp=737915754; 2025.

[7] The European Parliament. Directive (EU) 2023/2413 of the European parliament. https://eur-lex.europa.eu/eli/dir/2023/2413/oj.

[8] The European Parliament. Commission delegated regulation (EU) 2023/1184. https://eur-lex.europa.eu/eli/reg_del/2023/1184/oj/eng.

[9] Behrens J, Burger D. Atlas for suitable electrolyzer locations in Germany, H2PowerD -. www.ise.fraunhofer.de; 2025. https://www.h2-powerd.de/info/.

[10] Attiaoui M, Amrani SE, Silva HG, Neto J, Alami Merrouni A. Techno-economic and GIS mapping of wind-driven hydrogen production in Portugal. Int J Hydrogen Energy 2025;151. https://doi.org/10.1016/j.ijhydene.2025.150157.

[11] Seeger K, Genovese M, Schlüter A, Kockel C, Corigliano O, Díaz Canales EB, Praktiknjo A, Fragiacomo P. Techno-economic analysis of hydrogen and green fuels supply scenarios assessing three import routes: canada, Chile, and Algeria to Germany. Int J Hydrogen Energy 2025;116:558–76. https://doi.org/10.1016/j.ijhydene.2025.02.379.

[12] Télessy K, Barner L, Holz F. Repurposing natural gas pipelines for hydrogen: limits and options from a case study in Germany. Int J Hydrogen Energy 2024;80:821–31. https://doi.org/10.1016/j.ijhydene.2024.07.110.

[13] Wolf N, Tanneberger MA, Höck M. Levelized cost of hydrogen production in Northern Africa and Europe in 2050: a Monte Carlo simulation for Germany, Norway, Spain, Algeria, Morocco, and Egypt. Int J Hydrogen Energy 2024;69:184–94. https://doi.org/10.1016/j.ijhydene.2024.04.319.

[14] Alhadhrami K, Albalawi A, Hasan S, Elshurafa AM. Modeling green hydrogen production using power-to-x: saudi and German contexts. Int J Hydrogen Energy 2024;64:1040–51. https://doi.org/10.1016/j.ijhydene.2024.03.161.

[15] Eißler T, Groos U, Holst M, Deringer P, Edenhofer L, Mendler F, Voglstätter C, Szolak R. Optimizing the supply chain for green hydrogen and derivatives: a case study from Australia to Germany including inland transport considerations. Int J Hydrogen Energy 2025;144:1200–6. https://doi.org/10.1016/j.ijhydene.2025.04.163.

[16] Husarek D, Schmugge J, Niessen S. Hydrogen supply chain scenarios for the decarbonisation of a German multi-modal energy system. Int J Hydrogen Energy 2021;46:38008–25. https://doi.org/10.1016/j.ijhydene.2021.09.041.

[17] Jung C, Nagel L, Schindler D, Grau L. Fossil fuel reduction potential in Germany's transport sector by wind-to-hydrogen. Int J Hydrogen Energy 2018;43:23161–7. https://doi.org/10.1016/j.ijhydene.2018.10.181.

[18] McKenna R, Pfenninger S, Heinrichs H, Schmidt J, Staffell I, Bauer C, Gruber K, Hahmann AN, Jansen M, Klingler M, Landwehr N, Larsén XG, Lilliestam J, Pickering B, Robinius M, Tröndle T, Turkovska O, Wehrle S, Weinand JM, Wohland J. High-resolution large-scale onshore wind energy assessments: a review of potential definitions, methodologies and future research needs. 2022.

[19] Davis NN, Badger J, Hahmann AN. The global wind atlas: a high-resolution dataset of climatologies and associated web-based application. Bull Am Meteorol Soc 2023;104:E1507–25. https://doi.org/10.1175/BAMS-D-21-0075.1.

[20] Esri M. 10m annual land cover (2017–2023). https://www.arcgis.com/home/item.html?id=cfcb7609de5f478eb7666240902d4d3d; 2024.

[21] UNEP-WCMC, Heather Bingham, Deguignet M, Lewis E. User manual for the world database on protected areas and world database on other effective area-based conservation measures: 1.6 - (2019). http://wcmc.io/WDPA_Manual.

[22] EuroGeographics AISBL. OME2 EuroDEM - pan-european height dataset at medium scale -. https://eurogeographics.org/; 2023.

[23] Copernicus Climate Change Service. Climate and energy indicators for Europe from 1979 to present derived from reanalysis. Copernicus Climate Change Service (C3S) Climate Data Store (CDS) 2020. https://doi.org/10.24381/cds.4bd77450. 2025.

[24] Villanueva D, Feijóo A. A review on wind turbine deterministic power curve models. Appl Sci 2020;10:1–15. https://doi.org/10.3390/APP10124186.

[25] Badger J, Davis N, Hahmann A. The global wind atlas, an EUDP project carried out by DTU wind energy final report. 2015. p. 64011. 0347.

[26] Troen I, Lundtang Petersen E. European wind atlas. 1989. ISBN 87-550-1482-8.

[27] Lecanu PN, Bréard J, Mouazé D. Theoretical calculation of wind (or water) turbine considering kinetic and potential energy to exceed the Betz limit - hal open science hal-01982516v12. 2023.

[28] Masseran N. Evaluating wind power density models and their statistical properties. Energy 2015;84:533–41. https://doi.org/10.1016/j.energy.2015.03.018.

[29] Richter P, Wolters J, Frank M. Uncertainty quantification of offshore wind farms using Monte Carlo and sparse grid. Energy Sources B Energy Econ Plann 2022;17. https://doi.org/10.1080/15567249.2021.2000520.

[30] Dai J, Liu D, Wen L, Long X. Research on power coefficient of wind turbines based on SCADA data. Renew Energy 2016;86:206–15. https://doi.org/10.1016/j.renene.2015.08.023.

[31] Castillo OC, Andrade VR, Rivas JJR, González RO. Comparison of power coefficients in wind turbines considering the tip speed ratio and blade pitch angle. Energies 2023;16. https://doi.org/10.3390/en16062774.

[32] Landini S. Literature review: wind farm availability and power performance efficiency variability over life time. Heriot Watt University; 2016. 299073789.

[33] Sunder Selwyn T, Kesavan R. Availability analysis of wind turbines and its sub assemblies with Markov analysis at uncertain wind. Adv Sci Lett 2013;19:2210–4. https://doi.org/10.1166/asl.2013.4898.
[34] Ghaisas NN, Ghate AA, Lele SS. Effect of tip spacing, thrust coefficient and turbine spacing in multi-rotor wind turbines and farms. Wind Energy Science 2020;5: 51–72. https://doi.org/10.5194/wes-5-51-2020.
[35] Yadav S, Veeravalli SV, Singh SN. Effect of rotor spacing, overlapping and non-overlapping, on the performance of a coupled counter-rotating twin-rotor VAWT using CFD. Renew Energy 2024;221. https://doi.org/10.1016/j.renene.2023.119811.
[36] IREAN. Hydrogen from renewable power, technology outlook for the energy transition -. https://www.irena.org/publications; 2018.
[37] US department of energy: Hydrogen and fuel cell technologies office, multi-year program plan -. https://www.energy.gov/sites/default/files/2024-05/hfto-mypp-2024.pdf; 2024.
[38] Wang CR, Stansberry JM, Mukundan R, Chang HMJ, Kulkarni D, Park AM, Plymill AB, Firas NM, Liu CP, Lang JT, Lee JK, Tolouei NE, Morimoto Y, Wang CH, Zhu G, Brouwer J, Atanassov P, Capuano CB, Mittelsteadt C, Peng X, Zenyuk IV. Proton exchange membrane (PEM) water electrolysis: Cell-level considerations for gigawatt-scale deployment. 2025.
[39] Desai H, Heck T, Sacchi R, Schneider S, Terlouw T, Treyer K, Zhang X, Bauer C. Stromspeicherung und Wasserstoff-Technologien. Kosten und Auswirkungen auf das Klima Electricity storage and hydrogen-technologies, costs and impacts on climate change Including updates of costs and potentials of photovoltaics and wind power in Switzerland. 2022.
[40] Sobol IM. Global sensitivity indices for nonlinear mathematical models and their Monte Carlo estimates. Math Comput Simulat 2001;55:271–80. ISBN 03784754/01. Elsevier Science.
[41] Saltelli A. Making best use of model evaluations to compute sensitivity indices, vol. 145. 00104655/02. Elsevier Science, Computer Physics Communications; 2002. p. 280–97.
[42] Casas Ferrús MN, Ruhnau O, Madlener R. Portfolio effects in green hydrogen production under temporal matching requirements. Energy Strategy Rev 2024;56. https://doi.org/10.1016/j.esr.2024.101580.
[43] Breitschopf B, Alexander-Haw A. Auctions, risk and the WACC. How auctions and other risk factors impact renewable electricity financing costs. Energy Strategy Rev 2022;44. https://doi.org/10.1016/j.esr.2022.100983.
[44] Reksten AH, Thomassen MS, Møller-Holst S, Sundseth K. Projecting the future cost of PEM and alkaline water electrolysers; a CAPEX model including electrolyser plant size and technology development. Int J Hydrogen Energy 2022;47:38106–13. https://doi.org/10.1016/j.ijhydene.2022.08.306.
[45] International Energy Agency (IEA). Global hydrogen review 2025. Paris: IEA; 2025. Available from: https://iea.blob.core.windows.net/assets/a6c466dd-b6f0-44bd-a60a-6940eccfb1c3/GlobalHydrogenReview2025.pdf.
[46] European clean hydrogen alliance transmission and distribution roundtable: implementation of supply corridors. European Clean Hydrogen Alliance -; 2024. https://www.entsog.eu/sites/default/files/2024-11/ECH2A_Transmission%20Distribution%20Roundtable_Learnbook%20on%20Implementation%20of%20Hydrogen%20Supply%20Corridors.pdf.
[47] Bundesnetzagentur. Hydrogen core network -. https://www.bundesnetzagentur.de/EN/Areas/Energy/HydrogenCoreNe; 2024.
[48] Eurostat: Eurostat, Territorial units for statistics (NUTS), https://ec.europa.eu/eurostat/web/gisco/geodata/statistical-units/territorial-units-statistics.
[49] Demir G, Riaz M, Deveci M. Wind farm site selection using geographic information system and fuzzy decision making model. Expert Syst Appl 2024;255. https://doi.org/10.1016/j.eswa.2024.124772.
[50] Prognos AG, Öko-Institut e.V., Wuppertal Institut. Klimaneutrales Deutschland 2045 – Wie Deutschland seine Klimaziele schon vor 2050 erreichen kann. Berlin: Stiftung Klimaneutralität, Agora nergiewende, Agora Verkehrswende; 2021.
[51] Boston Consulting Group (BCG), Bundesverband der Deutschen ndustrie (BDI). Klimapfade 2.0 – ein Wirtschaftsprogramm für Klima und Zukunft. 2021. Berlin.
[52] Federal Ministry for Economic Affairs and Climate Action (BMWK). System development strategy 2024. Berlin: BMWK; 2024.
[53] 50Hertz Transmission GmbH, Amprion GmbH, TenneT TSO GmbH, TransnetBW GmbH. Netzentwicklungsplan strom 2037/2045, version 2025, 1. Entwurf. 2024. Berlin.
[54] Quentin J. Status of onshore wind energy development in Germany -. www.fachagentur-wind-solar.de; 2024.